Dalton Transactions

Trinuclear coordination assemblies of low-spin dicyano manganese(II) (S = 1/2) and iron(II) (S = 0) phthalocyanines with manganese(II) acetylacetonate and tris(cyclopentadienyl)gadolinium(III) and neodymium(III)

Journal:	*Dalton Transactions*
Manuscript ID	DT-ART-04-2022-001052.R2
Article Type:	Paper
Date Submitted by the Author:	31-May-2022
Complete List of Authors:	Romanenko, Nikita; Moscow State University Kuzmin, Alexey; Institute of Solid State Physics RAS, Mikhailenko, Maxim; FSBIS IPCP RAS Faraonov, Maxim; Institute of Problems of Chemical Physics of RAS, ; Institute of Problems of Chemical Physics Khasanov, Salavat; Institute of Solid State Physics RAS, Yudanova, Evgeniya; Institute of Problems of Chemical Physics RAS, Shestakov, Alexander; Institute of Problems of Chemical Physics RAS Yamochi, Hideki; Kyoto University, Division of Chemistry in Graduate School of Science Kitagawa, Hiroshi; Kyoto University, Department of Chemistry Otsuka, Akihiro; Kyoto University - Yoshida Campus, Department of Chemistry; Research Center for Low Temperature and Materials Sciences Konarev, Dmitri; Institute of Problems of Chemical Physics RAS, Department of Kinetics and Catalysis

ARTICLE

Trinuclear coordination assemblies of low-spin dicyano manganese(II) (*S* = 1/2) and iron(II) (*S* = 0) phthalocyanines with manganese(II) acetylacetonate and tris(cyclopentadienyl)gadolinium(III) and neodymium(III)

Received 00th January 20xx,
Accepted 00th January 20xx

DOI: 10.1039/x0xx00000x

Nikita R. Romanenko,[a] Alexey V. Kuzmin,[b] Maxim V. Mikhailenko,[a] Maxim A. Faraonov,[a] Salavat S. Khasanov,[c] Evgeniya I. Yudanova,[a] Alexander F. Shestakov,[a] Akihiro Otsuka,[c, d] Hideki Yamochi,[c, d] Hiroshi Kitagawa,[c] and Dmitri V. Konarev[a*]

Reaction of $Mn^{II}Pc$, $Fe^{II}Pc$ or $Fe^{II}PcCl_{16}$ with KCN in the presence of cryptand[2.2.2] yielded dicyano-complexes $\{Cryptand(K^+)\}_2\{M^{II}(CN)_2(macrocycle^{2-})\}^{2-}\cdot XC_6H_4Cl_2$ (M = Mn and Fe, X = 1 and 2) that were used for the preparation of trinuclear assemblies of general formula $\{Cryptand(K^+)\}_2\{M^{II}(CN)_2Pc\cdot(ML)_2\}^{2-}\cdot nC_6H_4Cl_2$ (M^{II} = Mn^{II}, Fe^{II}; n = 1, 4 and 5). These assemblies were formed via coordination of two manganese(II) acetylacetonate (ML = $Mn^{II}(acac)_2$, *S* = 5/2), tris(cyclopentadienyl)gadolinium (ML = Cp_3Gd^{III}, *S* = 7/2) or tris(cyclopentadienyl)neodymium (ML = Cp_3Nd^{III}, *S* = 3/2) units to nitrogen atoms of bidentate cyano ligands. The N(CN)-Mn{$Mn^{II}(acac)_2$} bond is 2.129(3) Å long but the bonds are elongated to 2.43-2.49 Å for tris(cyclopentadienyl)lanthanides. $\{Cryptand(K^+)\}_2\{Mn^{II}(CN)_2Pc\cdot(Mn^{II}(acac)_2)_2\}^{2-}\cdot 5C_6H_4Cl_2$ (2) contains three Mn(II) ions in different spin states (*S* = 5/2 and 1/2). Strong antiferromagnetic coupling of spins observed between them with exchange interaction (*J*) of -17.6 cm^{-1} providing the formation of high *S* = 9/2 spin state for $\{Mn^{II}(CN)_2Pc\cdot(Mn^{II}(acac)_2)_2\}^{2-}$ dianions at 2 K. Estimated exchange interaction between Mn^{II} (*S* = 1/2) and Gd^{III} (*S* =7/2) spins in $\{Mn^{II}(CN)_2Pc\cdot(Cp_3Gd^{III})_2\}^{2-}$ is only -1.1 cm^{-1}, and in contrast to **2**, nearly independent Gd^{III} and Mn^{II} centers are formed. As a result, no transition to the high-spin state is observed in these dianions. The $\{Mn^{II}(CN)_2Pc\cdot(Cp_3Nd^{III})_2\}^{2-}$ and$\{Fe^{II}(CN)_2Pc\cdot(Cp_3Nd^{III})_2\}^{2-}$ dianions with Cp_3Nd^{III} show the decrease of $\chi_M T$ values in the whole studied temperature range (300-1.9 K). Similar behaviour was found previously for pristine Cp_3Nd^{III} and $Cp_3Nd^{III}\cdot L$ complexes (L = alkylisocyanide ligand).

Introduction

Metallophthalocyanines (MPcs) present a large family of compounds which are used as dyes, sensors and materials for electronic and photoelectronic devices and solar cells.[1,2] Due to stacked or layered arrangement in the crystals MPcs can show high conductivity by partial oxidation of the macrocycles. Partial oxidation of $\{Fe^{III}(CN)_2(Pc^{2-})\}^-$ yields a compound showing giant magnetoresistance. In this case the interaction of conducting π-electrons delocalized over the macrocycles with *d*-electrons located on Fe^{III} atoms (*S* = 1/2) occurs providing the effect of magnetic field on conductivity.[3] MPcs can also be used as building blocks in the design of assemblies with promising optical and magnetic properties. Indigo and thioindigo dianions coordinate to central metal atoms of MPcs thereby combining phthalocyanine and organic dye in one molecule[4]. Such assemblies can show thermoinduced charge transfer between ligands[5]. Magnetic properties of MPcs can be modified by an addition of metal-containing fragments bearing heteroatoms or cyano-ligands to central metal atoms of MPcs. The examples of such fragments are $\{CpFe^{III}(dppe)CN\}^+$, $\{CpRu^{III}(dppe)CN\}^+$, $\{CpCo^{III}[(MeO)_2PO^-]_3\}^-$ and others.[6] Another promising way is an addition of metal-containing fragments to tin(II) or indium(III) phthalocyanines. This coordination is possible due to the formation of stable Sn(In)-M σ-bonds. In this case unpaired electrons are positioned either on the radical trianion $Pc^{\bullet 3-}$ macrocycles or coordinated metal atoms (M). Different fragments (M) can be attached as follows: $Fe(CO)_4$, $CpMo(CO)_2$, Cp^*RhCl_2, Cp^*IrCl_2, $CpFe(CO)_2$, $Ru_3(CO)_{11}$, $Os_3(CO)_{10}Cl$ and others.[7]

[a] *Institute of Problems of Chemical Physics RAS, Chernogolovka, Moscow region, 142432 Russia;*
[b] *Institute of Solid State Physics RAS, Chernogolovka, Moscow region, 142432 Russia;*
[c] *Division of Chemistry, Graduate School of Science, Kyoto University, Sakyo-ku, Kyoto 606-8502, Japan;*
[d] *Research Center for Low Temperature and Materials Sciences, Kyoto University, Sakyo-ku, Kyoto 606-8501, Japan.*

Electronic Supplementary Information (ESI) available: Supporting Information is available free of charge on the website. Experimental section including materials, general, synthesis and X-ray crystal structure determination, IR spectra of starting compounds and **1**-**8**, UV-visible-NIR spectra of **5** and **6**, crystal structures of **2**, **3** and **7**, **8**, details of magnetic measurements for **1-4, 6, 7** and results of theoretical calculations for **1** and **2**. See DOI: 10.1039/x0xx00000x

In this work dicyano complexes of manganese(II) and iron(II) phthalocyanines as well as iron(II) hexadecachlorophthalocyanine have been obtained and studied. Such complexes are known for manganese(II)[8] and (III)[9], as well as iron(II) and (III) phthalocyanines[10] but they have not been investigated for iron(II) hexadecachlorophthalocyanine so far. In this work we present for the first time temperature dependent EPR and SQUID measurements for the $\{Mn^{II}(CN)_2Pc\}^{2-}$ dianions. The $\{M^{II}(CN)_2Pc\}^{2-}$ dianions are used to obtain trinuclear assemblies $\{M^{II}(CN)_2Pc\cdot(ML)_2\}^{2-}$ with two manganese(II) acetylacetonate, tris(cyclopentadyenyl)gadolinium(III) or neodymium(III) as metal-containing ML units. Essential antiferromagnetic coupling between high- (S = 5/2) and low- (S = 1/2) spin manganese(II) atoms in $\{Mn^{II}(CN)_2Pc\cdot[Mn^{II}(acac)_2]_2\}^{2-}$ provides a transition of these units to high-spin (S = 9/2) state. Compounds with the $\{Mn^{II}(CN)_2Pc\cdot(Cp_3Gd^{III})_2\}^{2-}$, $\{Mn^{II}(CN)_2Pc\cdot(Cp_3Nd^{III})_2\}^{2-}$ and $\{Fe^{II}(CN)_2Pc\cdot(Cp_3Nd^{III})_2\}^{2-}$ dianions have also been obtained and studied for the first time to compare cyano-bridged assembies with d- and f-metals. Properties of $\{M^{II}(CN)_2Pc\}^{2-}$ and $\{Mn^{II}(CN)_2Pc\cdot[Mn^{II}(acac)_2]_2\}^{2-}$ dianions are discussed involving DFT calculations.

Results and discussion

a. Synthesis.

Cyanation of pristine $Mn^{II}Pc$, $Fe^{II}Pc$ and $Fe^{II}PcCl_{16}$ phthalocyanines was carried out by mixing of MPcs with an excess of KCN in the presence two equivalents of cryptand[2.2.2] in *o*-dichlorobenzene in anaerobic conditions. After one day of stirring at 60°C phthalocyanines were completely dissolved to form deep red-violet solution for $Mn^{II}Pc$ and deep green solutions for Fe(II)-containing phthalocyanines. To determine unit cell parameters for dicyano complexes we prepared their single crystals by slow mixing of the obtained solutions with *n*-hexane. Complexes **1** (M = Mn^{II}) and **5** (M = Fe^{II}) were found to be isostructural to previously studied complex $\{Cryptand(K^+)\}_2\{Sn^{IV}(CN)_2(Pc^{4-})\}^{2-}\cdot C_6H_4Cl_2$[11]. Elemental analysis of **1** supports the $\{Cryptand(K^+)\}_2\{Mn^{II}(CN)_2Pc\}^{2-}\cdot C_6H_4Cl_2$ composition which is similar to that of $\{Cryptand(K^+)\}_2\{Sn^{IV}(CN)_2(Pc^{4-})\}^{2-}\cdot C_6H_4Cl_2$. Crystal structure of isostructural complex **5** was determined from X-ray diffraction on single crystal (Fig. S14) to be $\{Cryptand(K^+)\}_2\{Fe^{II}(CN)_2Pc\}^{2-}\cdot 0.72C_6H_4Cl_2$. Structure of ~~a~~ the dicyano complex of iron(II) hexadecachlorophthalocyanine was also determined from X-ray diffraction analysis on single crystal (Table 1).

Furthermore, we studied the reaction of the $\{Mn^{II}(CN)_2Pc\}^{2-}$ dianions with two equivalents of metal acetylacetonates or tris(cyclopentadienyl)lanthanides in anaerobic conditions. Products were crystallized by slow mixing of the obtained solution with *n*-hexane allowing one to obtain single crystals suitable for X-ray diffraction analysis. Crystals with new unit cell parameters were obtained for **2**-**4** indicating the formation of new phases with trinuclear assemblies. In this case, the change in the solution color from red-violet to green was observed. In the case of (*iso*-Pr-Cp)$_3Dy^{III}$ or cobalt(II) acetylacetonate, only crystals of the starting dicyano complex were isolated, and no change in color of the solutions was found.

Table 1. Composition of the obtained complexes.

N	Composition
1	$\{Cryptand(K^+)\}_2\{Mn^{II}(CN)_2Pc\}^{2-}\cdot C_6H_4Cl_2$
2	$\{Cryptand(K^+)\}_2\{Mn^{II}(CN)_2Pc\cdot(Mn^{II}(acac)_2)_2\}^{2-}\cdot 5C_6H_4Cl_2$
3	$\{Cryptand(K^+)\}_2\{Mn^{II}(CN)_2Pc\cdot(Cp_3Gd^{III})_2\}^{2-}\cdot 4C_6H_4Cl_2$
4	$\{Cryptand(K^+)\}_2\{Mn^{II}(CN)_2Pc\cdot(Cp_3Nd^{III})_2\}^{2-}\cdot 4C_6H_4Cl_2$
5	$\{Cryptand(K^+)\}_2\{Fe^{II}(CN)_2Pc\}^{2-}\cdot 0.72C_6H_4Cl_2$
6	$\{Cryptand(K^+)\}_2\{Fe^{II}(CN)_2Pc\cdot(Cp_3Nd^{III})_2\}^{2-}\cdot 4C_6H_4Cl_2$
7	$\{Cryptand(K^+)\}_2\{Fe^{II}(CN)_2PcCl_{16}\}^{2-}\cdot 2C_6H_4Cl_2$
8	$\{Cryptand(K^+)\}_2\{Fe^{II}(CN)_2(PcCl_{16})\cdot(Cp_3Nd^{III})_2\}^{2-}\cdot C_6H_4Cl_2$

b. Crystal structures.

Geometry of $\{Mn^{II}(CN)_2Pc\}^{2-}$ has been studied in **2** and **3** whereas that of $\{Fe^{II}(CN)_2(PcCl_{16})\}^{2-}$ has been studied in **7**. Molecular structure of $\{Fe^{II}(CN)_2Pc\}^{2-}$ has also been solved in **5** but with rather low accuracy for bond lengths. Two cyano ligands coordinate to each metal atom in phthalocyanine (Fig. 1). In the case of $\{Mn^{II}(CN)_2Pc\}^{2-}$ four equatorial bonds are 1.951-1.955(3) Å but two Mn-C(CN) bonds are elongated to 2.013-2.018(3) Å (Table 2). Therefore, the Mn^{II} atoms have distorted octahedral environment. Similar geometry has been found for Fe^{II} atoms in $\{Fe^{II}(CN)_2PcCl_{16}\}^{2-}$ in which four short equatorial bonds of

Table 2. Bond lengths and angles for trinuclear assemblies studied in this work.

Coordination unit		N(CN)-M, Å	M	C(CN)-M(Pc), Å	C≡N, Å	M-N(CN)-C(CN), °	M(Pc)-N(Pc), Å	N_{meso}-C bonds (max/min length, Å)
$\{Mn^{II}(CN)_2Pc\cdot(Mn^{II}(acac)_2)_2\}^{2-}$	(**2**)	2.129(3)	Mn	2.013(3) Mn	1.156(3)	154.5(3)	1.955(3)	1.322(3) 1.328(3)
$\{Mn^{II}(CN)_2Pc\cdot(Cp_3Gd^{III})_2\}^{2-}$	(**3**)	2.433(2)	Gd	2.018(2) Mn	1.157(3)	151.5(3)	1.951(2)	1.322(3) 1.329(3)
$\{Cryptand(K^+)\}_2\{Fe^{II}(CN)_2PcCl_{16}\}^{2-}$	(**7**)	2.8747(15)	K	1.981(2) Fe	1.142(2)	147.0(3)	1.942(1)	1.320(2) 1.323(2)
$\{Fe^{II}(CN)_2(PcCl_{16})(Cp_3Nd^{III})_2\}^{2-}$	(**8**)	2.448(6) 2.491(6)	Nd Nd	1.977(7) Fe	1.143(5)	148.9(2)	1.949(5)	1.311(8) 1.328(8)

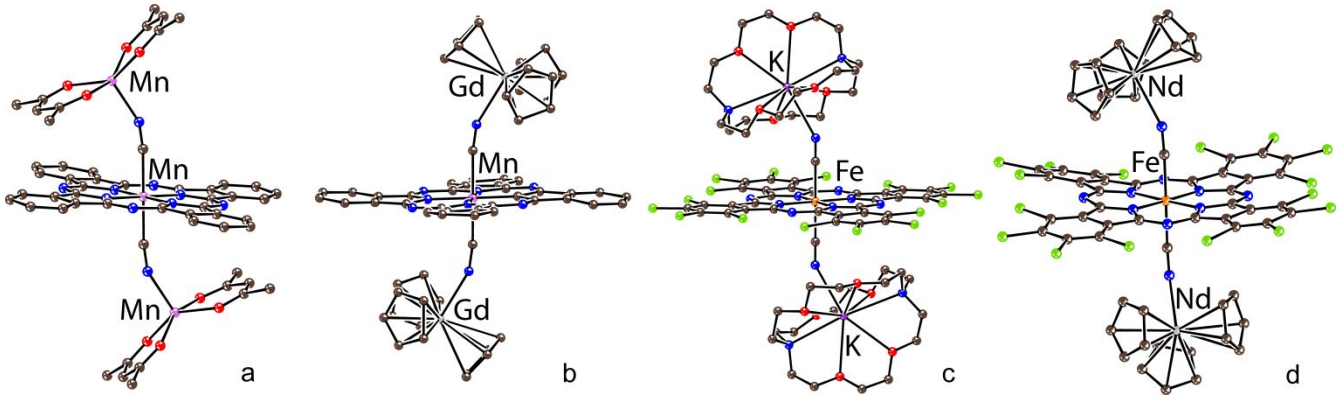

Fig. 1. Molecular structures of: (a) the $\{Mn^{II}(CN)_2Pc\cdot(Mn^{II}(acac)_2)_2\}^{2-}$ dianion in **2**; (b) the $\{Mn^{II}(CN)_2Pc\cdot(Cp_3Gd^{III})_2\}^{2-}$ dianion in **3**; (c) the neutral $\{Cryptand(K^+)\}_2\{Fe^{II}(CN)_2PcCl_{16}\}^{2-}$ assembly in **7**; (d) the $\{Fe^{II}(CN)_2(PcCl_{16})\cdot(Cp_3Nd^{III})_2\}^{2-}$ dianion in **8**.

1.942-1.949(5) Å and two longer Fe-C(CN) bonds of 1.977-1.981(2) Å are formed. Phthalocyanine macrocycles preserve dianionic state since alternation of N_{meso}-C bonds characteristic of radical trianion $Pc^{\bullet 3-}$ macrocycles[12] has not been found in **2** and **3** (Table 2). Bidentate cyano ligands in $\{Fe^{II}(CN)_2PcCl_{16}\}^{2-}$ have high affinity to metal centers since they coordinate to potassium ions in {cryptand[2.2.2](K^+)} (Fig. 1c). The K-N(CN) distance of 2.8747(15) Å is much shorter than the sum of van der Waals (vdW) radii of nitrogen and potassium atoms (4.22 Å)[13].

Metal atoms coordinate to nitrogen atoms of cyano ligands (Fig. 1). The shortest M-N(CN) bond of 2.129(3) Å length is formed with $Mn^{II}(acac)_2$. Longer M-N(CN) bonds are formed with Nd^{III} and Gd^{III} ions (2.43-2.49 Å, Table 2). In all cases coordination M-N(CN) bonds are positioned at an angle of 147-155° relative to linear NC-M-CN fragments, and total length of the assemblies is 10.2-10.8 Å. All assemblies are separated by bulky {Cryptand[2.2.2](K^+)} cations and solvent molecules (Fig. S13), and there are no direct π-π interactions between them. The shortest metal-metal distances for outer metal atoms from the adjacent assemblies are rather long being 6.25 for Nd^{III} in **8**, 6.87 for Gd^{III} in **3**, and 9.23 Å for Mn^{II} in **2**.

c. Optical properties.

Optical spectra of starting $Mn^{II}Pc$ and $Fe^{II}Pc$, and their dicyano complexes are shown in Fig. 2, whereas positions of peaks are listed in Table S5 in SI. Both $Mn^{II}Pc$ and $Fe^{II}Pc$ show spectra typical for metal(II) phthalocyanines with the Soret band at 349 and 326 nm and the Q-band at 690, 736 nm (split band) and 670 nm, respectively. Cyanation does not affect noticeably spectrum of $Fe^{II}Pc$. Only narrowing of both Soret and Q- bands is observed (Fig. 2b). On the whole, the spectrum of the $\{Fe^{II}(CN)_2Pc\}^{2-}$ dianions in **5** is similar to those of previously studied $\{Fe^{II}(N\text{-MeIm})_2Pc\}^0$ (*N*-MeIm: *N*-methylimidazole) and $\{Fe^{II}(Py)_2Pc\}^0$ complexes with low-spin Fe^{II} (S = 0).[14] On the contrary, the spectrum of $Mn^{II}Pc$ is modified substantially at cyanation. Instead of the split Q-band of $Mn^{II}Pc$, two intense bands are observed in the spectrum of **1** at 660 and 805 mn (Fig. 2a). Multiple bands are also observed at 385, 400, 451, 495, 521 and 568 nm (Fig. 2a). All these changes show that formation of $\{Mn^{II}(CN)_2Pc\}^{2-}$ affects electronic structure of $Mn^{II}Pc$. Previously, new bands were also found in the spectrum of salt with $\{Mn^{II}(CN)_2Pc\}^{2-}$ obtained by the cyanation of $Mn^{II}Pc$ in acetone.[8] Pristine $Mn^{II}Pc$ has intermediate S = 3/2 spin

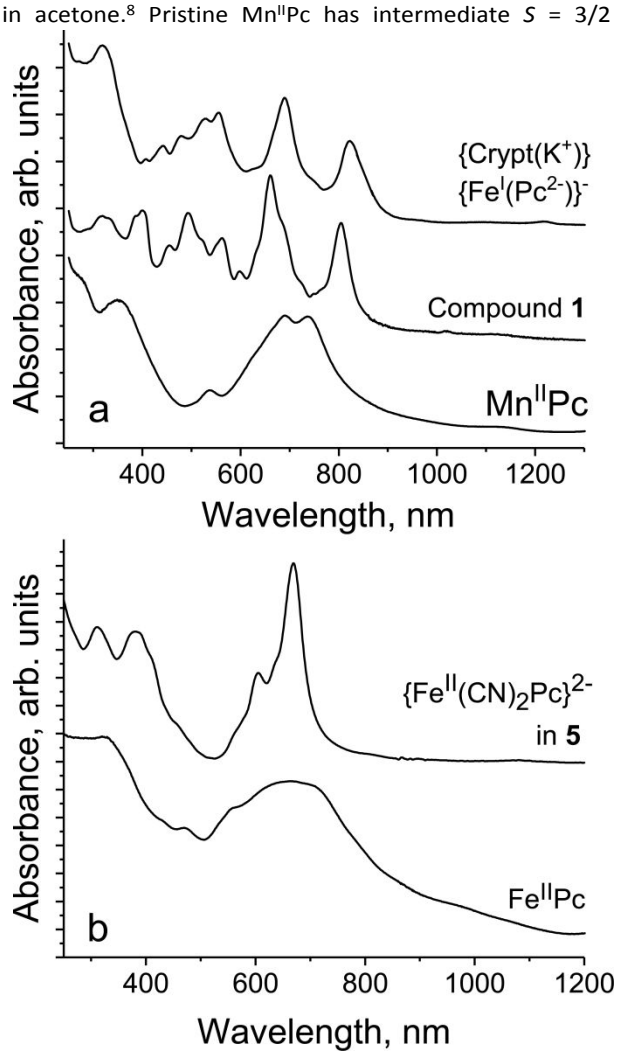

Fig. 2. UV-visible-NIR spectra of: (a) pristine $Mn^{II}Pc$ and (b) salt **1** with $\{Mn^{II}(CN)_2Pc\}^{2-}$ dianions and salt $\{Cryptand(K^+)\}\{Fe^{I}(Pc^{2-})\}^-\cdot C_6H_4Cl_2$ with low-spin (S = 1/2) $\{Fe^{I}(Pc^{2-})\}^-$ anions[17a]; (b) starting $Fe^{II}Pc$, and salt **5** with the $\{Fe^{II}(CN)_2Pc\}^{2-}$ dianions.

state.[15] This state is preserved when $Mn^{II}Pc$ forms complex with pyridine $\{Mn^{II}(Py)_2Pc\}^0$ or 1D polymer with 4,4`-bipyridyl $\{Mn^{II}(BPy)Pc\}_n$.[16] Optical spectra of these compounds support preservation of S = 3/2 spin state since they are similar to that of $Mn^{II}Pc$. Optical spectrum of $\{Mn^{II}(CN)_2Pc\}^{2-}$ supports lowering of spin state of Mn^{II} to S = 1/2 as it was observed previously[8]. It should be noted that the $\{Mn^{II}(CN)_2Pc\}^{2-}$ dianions in such configuration are isoelectronic to previously studied $\{Fe^{I}Pc\}^{-}$ anions containing Fe^{I} (S = 1/2).[17] Spectrum of $\{Cryptand(K^+)\}^+)\{Fe^{I}(Pc^{2-})\}^{-}\cdot C_6H_4Cl_2$[17a] shown in Fig. 2a is similar to that of **1** since it contains two intense bands at 688 and 822 nm, and multiple bands are manifested at 557, 526, 477, 442 and 406 nm. Both $\{M^{II}(CN)_2Pc\}^{2-}$ dianions (M = Mn^{II} and Fe^{II}) manifest a new band at 383-385 nm which is absent in the spectra of pristine phthalocyanines (Fig. 2).

The formation of assemblies does not affect noticeably the spectra of complexes containing dicyano iron(II) phthalocyanine dianions (Fig. S12 and Fig. 3b). However, coordination of metal fragments to $\{Mn^{II}(CN)_2Pc\}^{2-}$ affects its spectrum. First of all, splitting of the band at 660 nm into two bands (660 and 680 nm) is more pronounced in the spectra of **2**-**4**. An intense band at 568 nm observed in the spectrum of **1** disappears, whereas intense bands at 495 and 400 nm are blue shifted in the spectra of **2**-**4** to 473-482 and 383 nm, respectively (Fig. 3a).

IR spectra are shown in Figs. S1-S11, and positions of the peaks are listed in Tables S3 and S4. Three intense bands in the spectra of metal(II) phthalocyanines at 720-780 cm^{-1} are rather sensitive to charge state of Pc.[12] Cyanation shifts the most intense bands at 721 (Mn) and 731 cm^{-1} (Fe) to larger wavenumbers - 727 (Mn, **1**) and 734 cm^{-1} (Fe, **5**). Formation of radical trianion $Pc^{\bullet 3-}$ macrocycles shifts these bands to the opposite direction by 10-18 cm^{-1}.[12b] Therefore, coordination of two acceptor cyano ligands decreases electron density on the Pc macrocycles (the effect is opposite to the reduction). At the same time the bands attributed to the C≡N vibrations shift only slightly by 2-4 cm^{-1} at the formation of trinuclear assemblies indicating preservation of the C≡N bond length.

d. Magnetic properties.

I. Magnetic properties of $\{Mn^{II}(CN)_2Pc\}^{2-}$, $\{Fe^{II}(CN)_2Pc\}^{2-}$ and $\{Fe^{II}(CN)_2PcCl_{16}\}^{2-}$ dianions.

It is known that the $\{Mn^{II}(CN)_2Pc\}^{2-}$ dianions have the $\chi_M T$ value of 0.55 emu·K/mol indicating low-spin state (S = 1/2) of Mn^{II}.[8] We have analyzed temperature dependent magnetic characteristics of these dianions. The $\chi_M T$ value of 0.41 emu·K/mol at 300 K (Fig. 4) also corresponds to the low S = 1/2 spin state of $\{Mn^{II}(CN)_2Pc\}^{2-}$. Weiss temperature of -5 K (50-300 K) indicates weak antiferromagnetic intermolecular coupling of spins in **1** (Fig. S16). The $\chi_M T$ value only slightly decreases with temperature as shown in Fig. 4. Compound **1** manifests an intense asymmetric EPR signal in the spectrum measured for a polycrystalline sample in anaerobic conditions. It was fitted well by three Lorentzian lines with g_1 = 2.1116 (the linewidth ΔH = 8.12 mT), g_2 = 2.0746 (ΔH = 10.67 mT), g_3 = 1.9895 (ΔH = 24.33 mT) at 293 K (Fig. 5a). These components are slightly shifted and narrowed with temperature decrease down to 4.2 K: g_1 = 2.1029 (ΔH = 17.29 мТ), g_2 =2.0712 (ΔH = 9.65 mT) and g_3 =1.9907 (ΔH = 21.30 mT) (Fig. S18). The position of a signal also justifies low- (S = 1/2) spin state of Mn^{II}

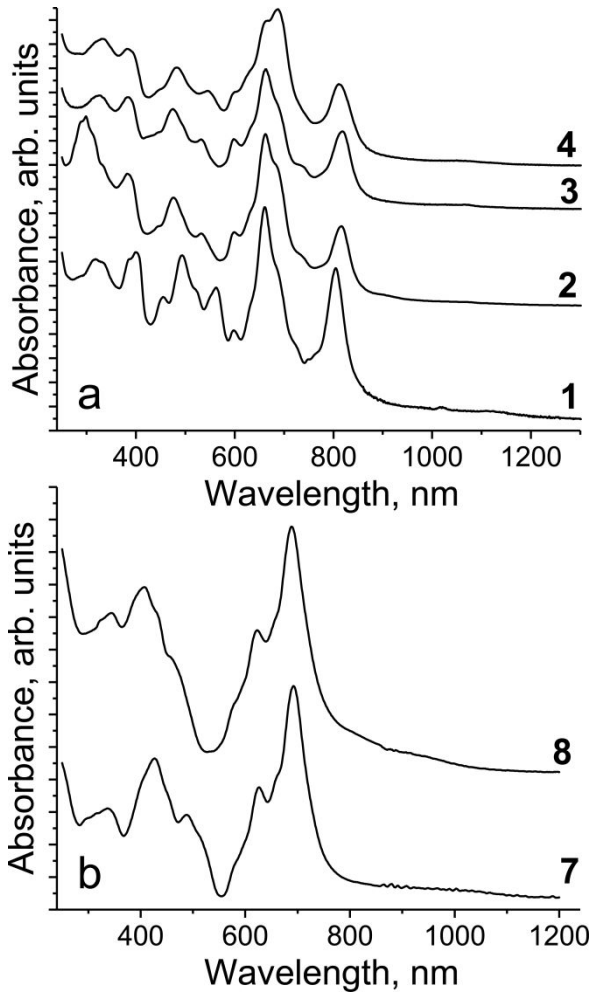

Fig, 3. UV-visible-NIR spectra of: (a) **1** with $\{Mn^{II}(CN)_2Pc\}^{2-}$ and corresponding complexes **2**, **3** and **4**; (b) **7** with $\{Fe^{II}(CN)_2PcCl_{16}\}^{2-}$ and corresponding complex **8**.

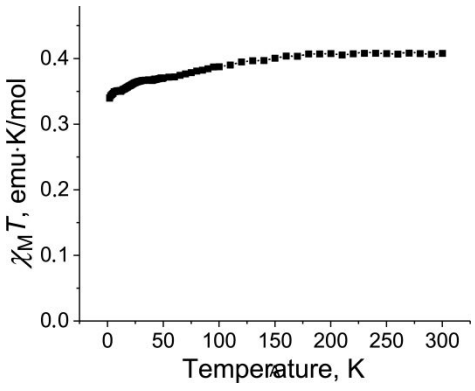

Fig. 4. Temperature dependence of $\chi_M T$ for **1** containing low-spin (S = 1/2) $\{Mn^{II}(CN)_2Pc\}^{2-}$ dianions.

in **1** since $Mn^{II}Pc$ in intermediate S = 3/2 spin state shows an asymmetric EPR signal with a low-field component at g = 4[16b].

Complexes **5** and **7** with the $\{Fe^{II}(CN)_2Pc\}^{2-}$ and $\{Fe^{II}(CN)_2PcCl_{16}\}^{2-}$ dianions have been studied by EPR technique at room and liquid helium temperatures, and **7** has also been analyzed by SQUID magnetometry. First of all, both complexes are EPR silent at these temperatures indicating singlet S = 0 spin state of the dianions. Molar magnetic susceptibility is negative and linear for **7** being χ_0 = -0.001376 emu/mol in the 50-300 K range (Fig. S36). The value of χ_0 calculated for **7** using Pascal constants is -0.001734 emu/mol. That also supports S = 0 state of $\{Fe^{II}(CN)_2PcCl_{16}\}^{2-}$. Estimated amount of Curie impurities for **7** is about 1.2% from the content of $Fe^{II}PcCl_{16}$.

II. Magnetic properties of trinuclear $\{Mn^{II}(CN)_2Pc\cdot(Mn^{II}(acac)_2)_2\}^{2-}$ assemblies in 2.

As we have shown, spin state of $\{Mn^{II}(CN)_2Pc\}^{2-}$ is S = 1/2 but manganese(II) acetylacetonate has a high-spin S = 5/2 state. As a result, the formation of a system of three independent S = 5/2, S = 1/2 and S = 5/2 spins is expected for **2** at high temperatures. The $\chi_M T$ value is 8.74 emu·K/mol at 300 K (Fig. 6, curve shown by open circles). The theoretically calculated value for such system is 9.12 emu·K/mol at g-factor = 2 that is close to the experimentally determined value. The $\chi_M T$ value

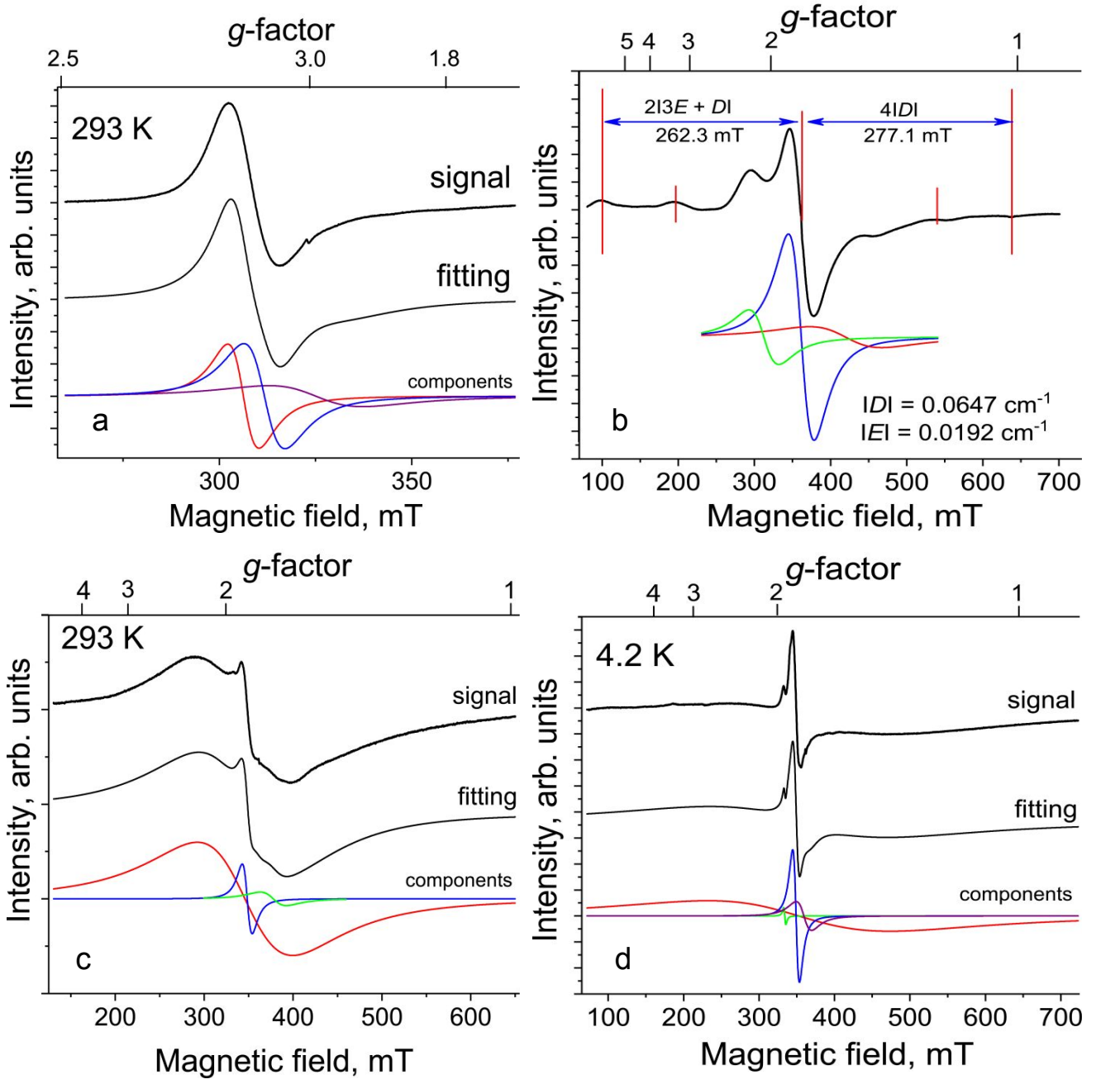

Fig. 5. Solid-state EPR spectra for the polycrystalline complexes measured in anaerobic conditions and their simulation: (a) **1** at 293 K; (b) **2** at 20 K (determination of ZFS parameters is also shown); **3** at 293 (c) and 4.2 K (d). Fitting of the signals by several Lorentzian lines is shown below the spectra.

decreases in the 50-300 K range, and Weiss temperature has been determined to be Θ = -12 K (Fig. S22) indicating antiferromagnetic coupling of spins. Magnetic behavior of **2** is modeled by PHI program[18] for three interacting Mn^{II} atoms in $\{Mn^{II}(CN)_2Pc\cdot(Mn^{II}(acac)_2)_2\}^{2-}$ with two *J* values as shown in Fig. 6. J_1 is for major Mn^{II} (*S* = 5/2) and Mn^{II} (*S* = 1/2) coupling and J_2 is for coupling between two boundary Mn^{II} (*S* = 5/2) centers located at a distance of 10.23 Å (Fig. 6). Exchange interaction J_1 = -17.6 cm^{-1} indicates strong antiferromagnetic coupling between high- and low-spin Mn^{II} atoms, whereas J_2 value is close to zero (-0.3 cm^{-1}) (-2*J* formalism, *g* = 2, Fig. 6). A small intermolecular coupling contribution of *zJ*' = 0.005 cm^{-1} is also taken into account (introduction of this parameter provides better correspondence between experimental and calculated curves in the 2-10 K range). Similarly, magnetic behavior of the assemblies of three high-spin (*S* = 5/2) Mn(II) atoms was previously modeled. In this case Mn^{II} atoms are bridged by oxygen atoms and the J_1 values in this case range from -2.1 to -2.9 cm^{-1}.[19]

Susceptibility increases below 40 K (Fig. 6) up to 11.60 emu·K/mol at 2 K. This increase can be explained by short-range magnetic ordering of spins within the assemblies since J_1 is relatively high in **2**. The value of 11.60 emu·K/mol observed at 2 K corresponds well to 12.37 emu·K/mol expected for the high *S* = 9/2 system at *g* = 2 when both *S* = 5/2 spins of Mn(II) are antiferromagnetically coupled with central *S* = 1/2 spin and, correspondingly, are ordered parallel to each other providing an *S* = 5/2 - 1/2 + 5/2 = 9/2 spin state. It is seen that an important condition for the manifestation of the high-spin state is a different spin state of central and outer Mn(II) atoms (*S* = 1/2 and *S* = 5/2). Field dependence of magnetization of **2** is shown in Fig. 7a. Magnetization is nearly saturated at 5T magnetic field at the value of 7.41 $N_A\mu_B$. No magnetic hysteresis is found for **2** at 2 K by susceptibility measurements in magnetic field between 5 and -5T.

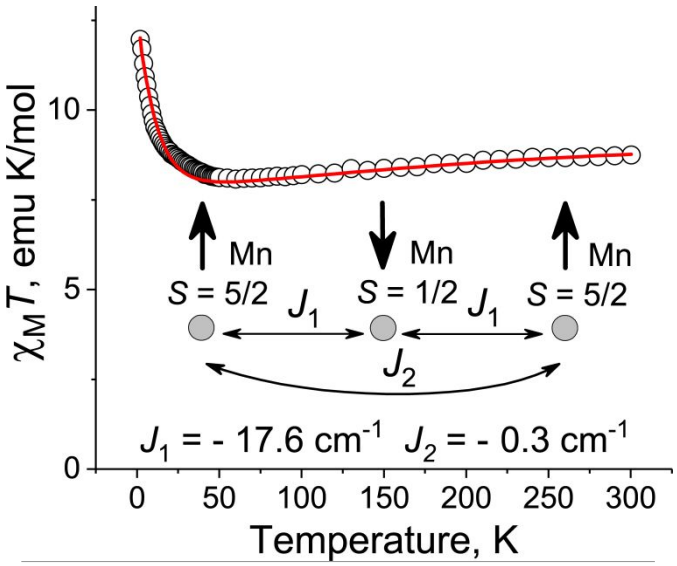

Fig. 6. Temperature dependence of χMT for {Cryptand(K+)}2{MnII(CN)2Pc·(MnII(acac)2)2}2·5C6H4Cl2 (2) in zero field cooling conditions and fitting of these data in the 2-300 K range by PHI program[18] (shown by red curve) .

Compound **2** shows an intense asymmetric EPR signal at room temperature which is fitted well by three Lorentzian lines. Parameters of these lines are g_1 = 2.0705 (ΔH = 39.2 mT), g_2 = 1.7892 (ΔH = 33.2 mT) and g_3 = 1.5410 (ΔH = 94.7 mT) at 20 K (Fig. 5b). Additional features of the EPR signal are manifested in **2** at higher and lower magnetic fields from the central three-component signal. These features can be attributed to zero-field splitting (ZFS) manifested for high-spin Mn(II) (*S* = 5/2) species. The following parameters can be determined: |*D*| = 0.0647, |*E*| = 0.0192 cm^{-1}, *E*/*D* = 0.298 and they are typical for high-spin Mn(II)[19, 20]. ZFS is not well resolved below 20 K.

c. Magnetic properties of trinuclear $\{Mn^{II}(CN)_2Pc\cdot(Cp_3Gd^{III})_2\}^{2-}$ assemblies in 3.

Cyano-bridged assemblies with tris(cyclopentadienyl)-lanthanides are still unknown, and trinuclear $\{Mn^{II}(CN)_2Pc\cdot(Cp_3Gd^{III})_2\}^{2-}$ assembly is a first example. There are two high-spin Gd^{III} atoms (*S* = 7/2) separated by a low-spin Mn(II) center (*S* = 1/2) in **3**. The $\chi_M T$ value is 15.01 emu·K/mol at 300 K (Fig 7). This value is close to that of the system with

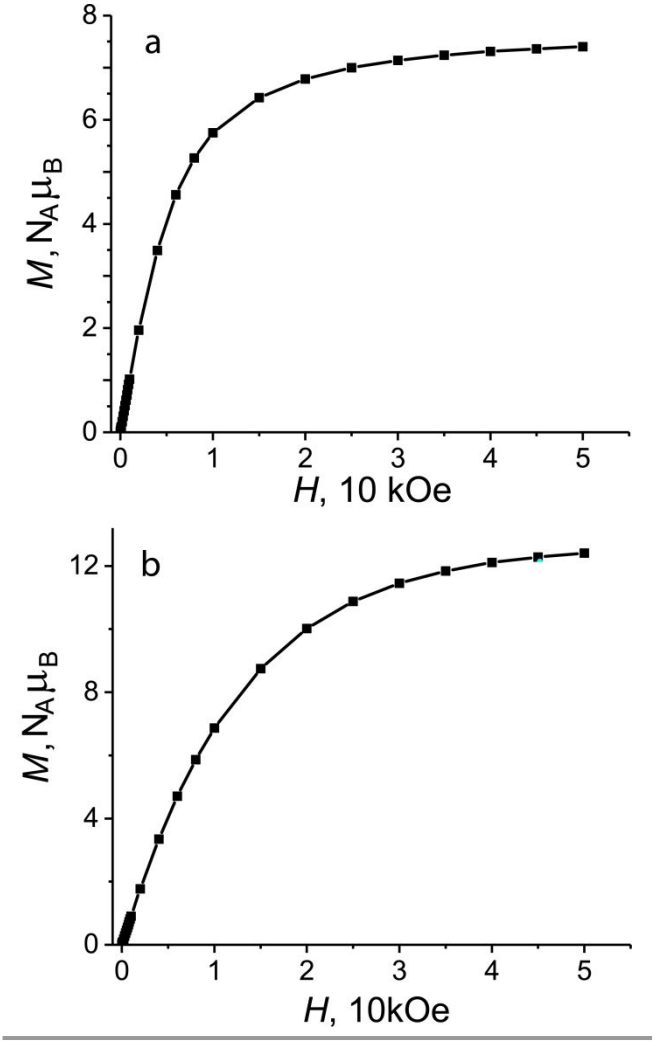

Fig.. **7**. Magnetization of **2** (a) and **3** (b) in $N_A\mu_B$ *vs* magnetic field up to 5T (black line is a guide to the eye)

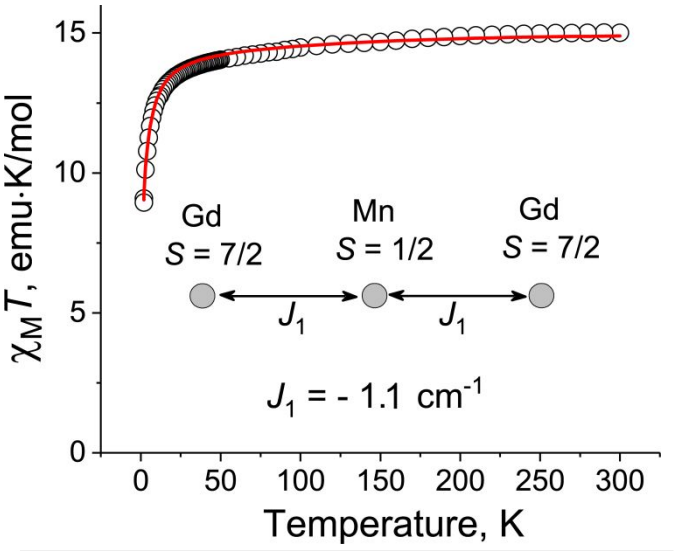

Fig. 8. (a) Temperature dependence of $\chi_M T$ for $\{Cryptand(K^+)\}_2\{Mn^{II}(CN)_2Pc\cdot(Cp_3Gd^{III})_2\}^{2-}\cdot 4C_6H_4Cl_2$ (**3**) and fitting of these data by PHI program[18] in the 1.9-300 K range (shown by red curve) .

three non-interacting S = 7/2, S = 1/2, S = 7/2 spins: 16.12 emu·K/mol at g = 2. The Gd^{III} atoms have $^8S_{7/2}$ ground state at g-factor of 2.[21]

Magnetic behavior of the trinuclear $MnGd_2$ assembly in **3** was modeled by PHI program[18] as well. A good agreement between experimental and theoretical curves is observed at very weak antiferromagnetic exchange interaction between Gd^{III} and Mn^{II} centers with J_1 = -1.1 cm^{-1} (Fig. 8). It is seen that this interaction is nearly 15 times weaker in comparison with that for **2**. Therefore, as observed previously, d-metals (Mn) provide essentially stronger magnetic coupling of spins in the cyano-bridged assemblies in comparison with f-metals (Gd). Weak coupling is also the reason of that the formation of high-spin species in not observed for **3**. Fitting for **3** was carried out at fixed g-factors of 1.84 for Mn^{II} and 1.90 for Gd^{III} which were directly extracted from the EPR spectra of 3. Zero-splitting parameter D for Gd^{III} is |0.9| cm^{-1}. Since the distance between Gd atoms from the adjacent $MnGd_2$ assemblies is 6.871 Å (Fig. S13a), a small intermolecular coupling contribution of zJ' = -0.02 cm^{-1} is also taken into account (introduction of this parameter provides better correspondence between experimental and calculated curves). The field dependence of magnetization of **3** is shown in Fig. 7b. Magnetization is not saturated even at 5T magnetic field reaching the value of 12.40 $N_A\mu_B$.

EPR spectrum of **3** at 293 K is shown in Fig. 5c. The signal contains a very wide and intense line at g_1 = 1.8699 and the linewidth of 107 mT and a substantially narrower and weaker two-component signal with g_2 = 1.7119 (ΔH = 29.4 mT), and g_3 = 1.8562 (ΔH = 11.02 mT) (Fig. 5c). Total integral intensity of the two-component narrow signal is only 2.5% from that of the wide signal and that corresponds approximately to relative contributions from two high-spin Gd^{III} atoms and low-spin Mn^{II} atoms. Therefore, the wide signal can be attributed to Gd^{III} but the narrow signal originates from Mn(II) (S = 1/2). The wide EPR signal expands greatly and shifts towards large g-factors with decreasing temperature (Figs. S28 and S29). Maximal linewidth of the signal (275 mT) at g = 1.89 is observed at 150 K, and below this temperature the signal shifts to smaller g-factors and only slightly narrows (g_1 = 1.8342 at the 242 mT linewidth, 4.2 K, Fig. 5d). The narrow signal can be fitted better by three lines at 4.2 K with g_2 = 1.7994 (20.54 mT), g_3 =1.8529 (8.90 mT), g_4 = 1.9359 (2.79 mT) (Fig. 5d). Observation of separate EPR signals from individual paramagnetic Gd^{III} and Mn^{II} species indicates weakness of magnetic coupling between them in the assemblies that is confirmed by the data obtained from SQUID magnetometry.

d. Magnetic properties of trinuclear $\{Mn^{II}(CN)_2Pc\cdot(Cp_3Nd^{III})_2\}^{2-}$ assemblies in 4.

The Nd^{III}-Mn^{II}-Nd^{III} assemblies contain two different paramagnetic centers. According to previous estimation, central Mn^{II} atom has low S = 1/2 spin state. The Nd^{III} atom in Cp_3Nd^{III} have $^4I_{9/2}$ ground state at g = 8/11. It has three 4f-electrons, and theoretical $\chi_M T$ value for Nd^{III} is expected to be 1.64 emu·K/mol.[21] However, experimentally this value is not achieved due to the population of excited states with lower total angular momentum values at room temperature.

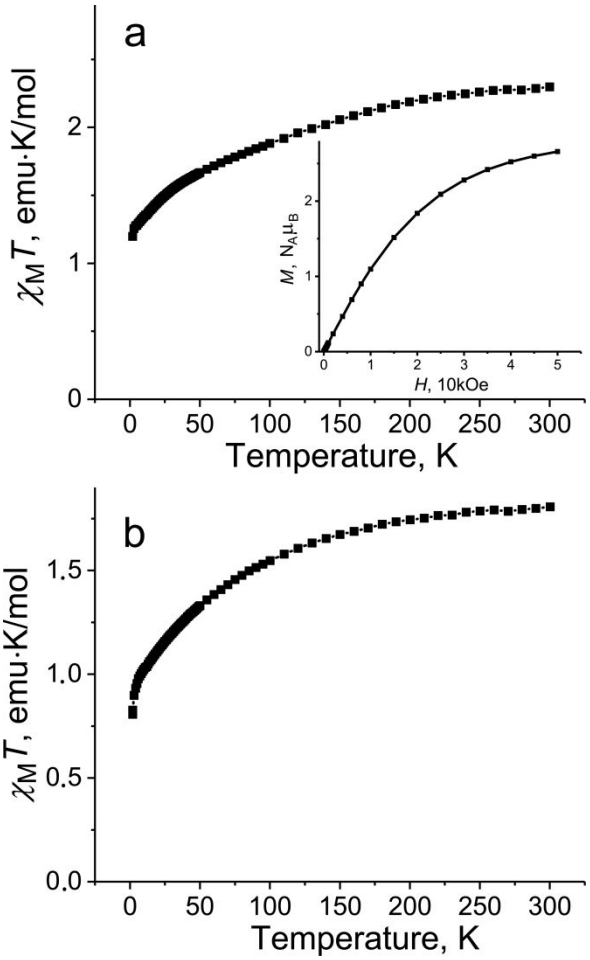

Fig. 9. Temperature dependencies of the $\chi_M T$ values for polycrystalline: **4** (a) and **6** (b). Inset for Fig. a shows magnetization of **4** in $N_A\mu_B$ *vs* magnetic field up to 5T (black line is a guide to the eye)

Previously magnetic properties of pristine Cp_3Nd^{III} as well as Cp_3Nd^{III} complexes with one alkylisocyanide ligand (L) were studied. The $\chi_M T$ values for pristine Cp_3Nd^{III} is 1.27 emu·K/mol at 300 K whereas the Cp_3Nd^{III}·L complexes show even smaller values being 0.95 emu·K/mol at 300 K. Moreover, the $\chi_M T$ value is not temperature independent even at 300 K and decreases in the 300-1.9 K range.[22] The $\chi_M T$ value for **4** is 2.30 emu·K/mol at 300 K which is also lower than expected (3.56 emu·K/mol) for three non-interacting centers: two Nd^{III} atoms in $^4I_{9/2}$ ground state and low-spin Mn^{II} ion (S = 1/2) (Fig 8a). This value decreases to 1.125 emu·K/mol at 1.9 K in the whole studied temperature range (300-1.9 K, Fig 8a). Similarly to Cp_3Nd^{III} and Cp_3Nd^{III}·L[22], this decrease can be attributed to the crystal field effects for Nd^{III} and additional contribution for **4** can be given also by weak antiferromagnetic coupling between the Nd^{III} and Mn^{II} centers within the assemblies. The compound with the $\{Fe^{II}(CN)_2Pc\cdot(Cp_3Nd^{III})_2\}^{2-}$ dianions (**6**) was also synthesized. In this case the Fe^{II} atoms in phthalocyanine are diamagnetic (S = 0), and the exchange through them is weaker due to a long distance between two Nd^{III} atoms (about 10.8 Å for isostructural **3**). Therefore, in contrast to **4**, magnetic behavior of **6** is defined mainly by the isolated $Cp_3Nd^{III}(NC)$ centers. The $\chi_M T$ value of 1.92 emu·K/mol at 300 K for **6** (Fig. 8b) is lower than that for **4** (Fig. 8a) justifying the presence of an additional paramagnetic center Mn^{II} (S = 1/2) in **4**. The $\chi_M T$ value decreases with temperature down to 0.75 emu·K/mol at 1.9 K (Fig. 8b), and such behavior is similar to those of **4**, Cp_3Nd^{III} and Cp_3Nd^{III}·L[21]. The field dependence of magnetization of **4** is shown in Fig. 9a, inset. Magnetization is not saturated even at 5T magnetic field reaching the value of 2.67 $N_A\mu_B$.

EPR spectrum of **4** was studied in the 293-4.2 K range. There are wide and narrow asymmetric EPR signals which can be fitted well by several Lorentzian lines at 293 K (Fig. S33). The wide signal can be fitted by three lines with g_1 = 2.0275 (ΔH = 28.80 mT), g_2 = 2.0836 (ΔH = 10.51 mT) and g_3 = 2.1167 (ΔH = 7.52) whereas the narrow signal is fitted by two lines with g_4 = 2.0039 (ΔH = 0.32 mT) and g_2 = 2.0022 (ΔH = 0.72 mT) (Fig. S33). The latter signal is too narrow to be attributed to $\{Mn^{II}(CN)_2Pc\}^{2-}$, and its integral intensity is less than 0.1% from that of the wide signal. Therefore, most probably this signal originates from Curie impurities localized on Pc, for example, reduced $Pc^{\bullet 3-}$radical trianions but the content of these species is too low to affect magnetic properties of **4**. The wide signal can originate from both Nd^{III} and Mn^{II} species. The signal is three-component, but exact attribution of these components is not possible. Here it should be noted that Cp_3Nd^{III}·L complexes can also show EPR signals in the same range of g-factors ($g_\perp$-component)[22b]. Temperature decrease preserves the same linewidth of the components of the wide signal but they are shifted to smaller g-factors: g_1 = 1.9740 (ΔH = 24.60 mT), g_2 = 2.0519 (ΔH = 11.63 mT) and g_3 = 2.0936 (ΔH = 8.97 mT) at 4.2 K (Fig. S33).

e. Theoretical calculations.

For an isolated atom or ion with an open d-shell, the maximum multiplicity is realized according to Hund's rule. Under the influence of the ligand environment, splitting of the d-orbitals occurs and the high-spin state of the $Mn^{II}Pc$ complex with macrocyclic ligand (Fig. S39) is not realized due to strong destabilization of the x^2-y^2 orbital. Only lower axial z^2 orbital is populated in the ground quartet state. The sextet and doublet states are higher in energy by 0.53 and 1.12 eV, respectively. Upon coordination of two axial cyano-ligands in $\{Mn^{II}(CN)_2Pc\}^{2-}$ (Fig. S39), relative energy of the z^2 orbital increases. Therefore, the low-spin doublet state of the $\{Mn^{II}(CN)_2Pc\}^{2-}$ complex is a ground state (Fig. 10), and quartet and sextet states are higher by 0.48 and 1.24 eV, respectively. For similar reasons, the $\{Fe^{II}(CN)_2Pc\}^{2-}$ dianion (Fig. S40) has a singlet ground state, and a triplet one is higher by 0.81 eV.

$Mn^{II}(acac)_2$ coordination to nitrogen atoms of cyano ligands has almost no effect on geometry of the central $\{Mn^{II}(CN)_2Pc\}^{2-}$ fragment (see Fig. S42). In this case, the charge on a cyano ligand decreases from -0.488 to -0.234. At the same time, comparable electron density transfer of -0.382 occurs mainly from the macrocycle since the charge on the central Mn^{II} atom changes only slightly from 0.171 to 0.153. A slight decrease in the Mn-C(CN) distance from 2.031 to 1.998 Å ~~at~~ upon coordination of $Mn^{II}(acac)_2$ can be attributed to the donor-acceptor transfer of electron density (-0.445) to each $Mn^{II}(acac)_2$ unit. The $\{Mn^{II}(CN)_2Pc\cdot(Mn^{II}(acac)_2)_2\}^{2-}$ dianions can have high- (S = 11/2) and low- (S = 9/2) spin states at parallel and antiparallel arrangement of spins of high- and low-spin Mn^{II} atoms. These states are nearly degenerated, and their relative energies are discussed in SI.

Conclusion

The dicyano complexes of $Mn^{II}Pc$, $Fe^{II}Pc$ and $Fe^{II}PcCl_{16}$ have been obtained. Central metal atoms decrease spin state to the lowest possible state (S = 1/2 for Mn^{II} and S = 0 for Fe^{II}-containing complexes). The formation of $\{Mn^{II}(CN)_2Pc\}^{2-}$ provides appearance of new bands in the visible and NIR ranges. As a result, their spectra show some similarities with optical spectrum of isoelectronic $\{Fe^{I}(Pc^{2-})\}^{-}$ anions. These dicyano complexes have been used for preparation of trinuclear assemblies with $Mn^{II}(acac)_2$ as well as Cp_3Gd^{III} and Cp_3Nd^{III}. It should be noted that tris(cyclopentadienyl)-lanthanides are used for preparation of cyano-bonded assemblies for the first time, and this approach opens a new

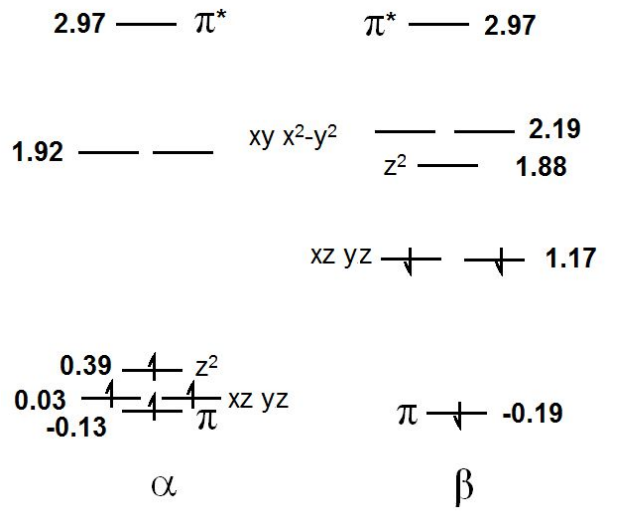

Fig. 10. Scheme of electronic levels calculated for the $\{Mn^{II}(CN)_2Pc\}^{2-}$ dianions. Energies are given in eV.

way for the development of lanthanide-containing assembles. Previously, mainly neutral ligands were coordinated to tris(cyclopentadienyl)gadolinium(III) and neodymium(III)[22b, 23]. Antiferromagnetic coupling of high-spin Mn^{II} (S = 5/2) with central low-spin Mn^{II} (S =1/2) orders spins of outer atoms parallel to each other producing high-spin S = 9/2 $\{Mn^{II}(CN)_2Pc\cdot(Mn^{II}(acac)_2)_2\}^{2-}$ dianions at 2 K. Previously, high-spin state was found for the assemblies of radical anions or trianions of substituted hexaazatriphenylenes with three paramagnetic metal centers like Co^{II} (S = 3/2) or Fe^{II} (S = 2). In this case spins of metal atoms are ordered parallel to each other when they couple antiferromagnetically with S = 1/2 spin of hexaazatriphenylenes.[24] This work shows that trinuclear assemblies containing metal ions in high- and low-spin states can also form similar high-spin species. They are promising building blocks to prepare compounds with long-range magnetic ordering of spins at their close packing in the crystals or to obtain combination of conductivity and magnetism when partially oxidized or reduced phthalocyanine macrocycles are formed in such assemblies. On the contrary, essentially weaker magnetic coupling is observed between high-spin gadolinium(III) and low-spin manganese(II) atoms in $\{Mn^{II}(CN)_2Pc\cdot(Cp_3Gd^{III})_2\}^{2-}$, and in this case high-spin species are not formed down to 1.9 K.

Conflicts of interest

There are no conflicts to declare.

Acknowledgements

The work for preparation and study of **1**-**6** was supported by Russian Science Foundation (project N 21-13-00221). Study of complexes **7** and **8** with iron(II) perchlorophthalocyanine was supported by Russian Science Foundation (project N 21-73-10207). Analysis of IR spectra of **1**, **5** and **7** was supported by the Ministry of Science and Higher Education of the Russian Federation (registration number AAAA-A19-119092390079-8). Some magnetic measurements were suported by JSPS KAKENHI Grant Number JP20K05448, and the JST (ACCEL) 27 (100150500019) project.

ORCID:

M.A. Faraonov: 0000-0003-0805-601X
A. Otsuka: 0000-0002-3141-0702
H. Yamochi: 0000-0002-0127-6530
H. Kitagawa: 0000-0001-6955-3015
D.V. Konarev: 0000-0002-7326-8118

Contribution of the authors:

N.R. Romanenko -Investigation
A.V. Kuzmin -Investigation
M.V. Mikhailenko - Investigation
M.A. Faraonov - Investigation
S.S. Khasanov -Investigation
E.I. Yudanova -Formal Analysis
A.F. Shestakov - Formal Analysis
A. Otsuka - Resources
H. Yamochi -Resources
H. Kitagawa -Project administration
D.V. Konarev -Supervision Investigation Writing – original draft

Notes and references

1 (a) T. Nyokong, *Coord. Chem. Rev*. 2007, **251**, 1707 − 1722; (b) D. Placencia, W. Wang, J. Gantz, J. L. Jenkins and N. R. Armstrong, *J. Phys. Chem. C*, 2011, **115**, 18873 – 18884; (c) C. G. Claessens, W. J. Blau, M. Cook, M. Hanack, R. J. M. Nolte, T. Torres and D. Wöhrle, *Monat. Chem.* 2001, **132**, 3 − 11; (d) O. I. Koifman, T. A. Ageeva, I. P. Beletskaya, A. D. Averin, A. A. Yakushev, L. G. Tomilova, T. V. Dubinina, A. Yu. Tsivadze, Yu. G. Gorbunova, A. G. Martynov, D. V. Konarev, S. S. Khasanov, R. N. Lyubovskaya et all, *Macroheterocycles,* 2020, **13**, 311 − 467.

2 (a) L. J. Boucher, Metal Complexes of Phthalocyanines. In: G. A. Melson (eds) Coordination Chemistry of Macrocyclic Compounds. Springer, Boston, MA, 1979, pp. 461 – 516; (b) I. Beletskaya, V. S. Tyurin, A. Y. Tsivadze, R. Guilard and C. Stern, *Chem. Rev.* 2009, **109**, 1659 – 1713; (c) V. N. Nemykin and E. A. Lukyanets, *ARKIVOC,* Arkat USA, Inc., 2010, 136 – 208. DOI: http://dx.doi.org/10.3998/ark.5550190.0011.104

3 (a) J. L. Petersen, C. S. Schramm, D. R. Stojakovic, B. M. Hoffman and T. J. Marks, *J. Am. Chem. Soc.* 1977, **99**, 286 – 288; (b) D. Ethelbhert, C. Yu, M. Matsuda, H. Tajima, A. Kikuchi, T. Taketsugu, N. Hanasaki, T. Naito and T. Inabe, *J. Mater. Chem.* 2009, **19**, 718 – 723; (c) M. Matsuda, N. Hanasaki, H. Tajima, T. Naito and T. Inabe, *J. Phys. Chem. Solids* 2004, **65**, 749 – 752; (d) T. Inabe and H. Tajima, *Chem. Rev.* 2004, **104**, 5503 – 5534.

4 D. V. Konarev, A. V. Kuzmin, A. M. Fatalov, S. S. Khasanov, E. I. Yudanova and R. N. Lyubovskaya, *Chem. Eur. J.* 2018, **24**, 8415 – 8423.

5 D. V. Konarev, L. V. Zorina, S. S. Khasanov, A. F. Shestakov, A. M. Fatalov, A. Otsuka, H. Yamochi, H. Kitagawa and R. N. Lyubovskaya, *Inorg. Chem*. 2018, **57**, 583 – 589.

6 (a) M. T. M. Choi, C.-F. Choi and D. K. P. Ng, *Tetrahedron*, 2004, **60**, 6889–6894; (b) J. Silver, J. L. Sosa-Sanchez and C. S. Frampton, *Inorg. Chem.* 1998, **37**, 411 – 417; (c) A. Geiss, H. Vahrenkamp, *Inorg. Chem.* 2000, **39**, 4029 – 4036; (d) H. Ke, W.-K. Wong, W.-Y. Wong, H.-L. Tam, C.-T. Poon and F. Jiang, *Eur. J. Inorg. Chem.* 2009, 1243 – 1247; (e) Y. Z. Voloshin, O. A. Varzatskii, S. V. Korobko, V. Y. Chernii, S. V. Volkov, L. A. Tomachynski, V. I. Pehn'o, M. Yu. Antipin and Z. A. Starikova, *Inorg. Chem.* 2005, **44**, 822 – 824; (f) S. V. Dudkin, A. S. Belov, Y. V. Nelyubina, A. V. Savchuk, A. A. Pavlov, V. V. Novikova, Y. Z. Voloshin, *New J. Chem*. 2017, **41**, 3251 – 3259; (g) A. Geiss, M. J. Kolm, C. Janiak and H. Vahrenkamp, *Inorg. Chem.* 2000, **39**, 4037 – 4043.

7 (a) D. V. Konarev, A. V. Kuzmin, Y. Nakano, M. A. Faraonov, S. S. Khasanov, A. Otsuka, H. Yamochi, G. Saito and R. N. Lyubovskaya, *Inorg. Chem.* 2016, **55**, 1390 – 1402; (b) D. V. Konarev, A. V. Kuzmin, M. S. Batov, S. S. Khasanov, A. Otsuka, H. Yamochi, H. Kitagawa and R. N. Lyubovskaya, *ACS Omega* 2018, **3**, 14875 – 14888; (c) N. R. Romanenko, A. V. Kuzmin, S. S. Khasanov, M. A. Faraonov, E. I. Yudanova, Y. Nakano, A. Otsuka, H. Yamochi, H. Kitagawa and D. V. Konarev, *Dalton Trans*, 2022, **51**, 2226 – 2237.

8 S. Sievertsen, H. Grunewald and H. Homborg, *Z. Anorg. Allg. Chem*., 1993, **619**, 1729 – 1737.

9 (a) A. P. Hansen and H. M. Goff, *Inorg. Chem.* 1984, **23**, 4519 – 4525; (b) M. Matsuda, J.-I. Yamaura, H. Tajima and T. Inabe, *Chem. Let*. 2005, **34**, 1524 – 1525.

10 (a) B. W. Dale, *Trans. Faraday Soc*. 1969, 331 – 338; (b) M. J. Stillman and A. J. Thomson, *J. Chem. Soc., Faraday Trans. 2*, 1974, **70**, 790–804; (c) T. Nyokong, *J. Chem. Soc. Dalton Trans*, 1993, 3601 – 3604; (d) M. Matsuda, T. Asari, T. Naito, T. Inabe, N. Hanasaki, and H.Tajima, *Bull. Chem. Soc. Jpn.* 2003, **76**, 1935 – 1940.

11 D. V. Konarev, A. V. Kuzmin, A. F. Shestakov, I. A. Rompanen

and R. N. Lyubovskaya, *Dalton Trans*, 2020, **49**, 16801 – 16812.

12 12 (a) J. A. Cissell, T. P. Vaid and A. L. Rheingold, *Inorg. Chem.* 2006, **45**, 2367 – 2369; (b) D. V. Konarev, A. V. Kuzmin, M. A. Faraonov, M. Ishikawa, Y. Nakano, S. S. Khasanov, A. Otsuka, H. Yamochi, G. Saito and R. N. Lyubovskaya, *Chem. Eur. J.* 2015, **21**, 1014 – 1028; (c) D. V. Konarev, M. A. Faraonov, A. V. Kuzmin, S. S. Khasanov, Y. Nakano, M. S. Batov, S. I. Norko, A. Otsuka, H. Yamochi, G. Saito and R. N. Lyubovskaya, *New J. Chem.* 2017, **41**, 6866 – 6874; (d) D. V. Konarev, A. V. Kuzmin, S. S. Khasanov, A. L. Litvinov, A. Otsuka, H. Yamochi, H. Kitagawa and R. N. Lyubovskaya, *Chem. Asian J.* 2018, **13**, 1552 – 1560; e). D. V. Konarev, A. V. Kuzmin, S. S. Khasanov, M. S. Batov, A. Otsuka, H. Yamochi, H. Kitagawa and R. N. Lyubovskaya, *CrystEngComm*. 2018, **20**, 385 – 401.

13 S. S. Batsanov, *Inorg. Mat.* 2001, **37**, 871 – 885.

14 (a) D. V. Konarev, A. V. Kuzmin, Y. Nakano, S. S. Khasanov, A. Otsuka, H. Yamochi, H. Kitagawa and R. N. Lyubovskaya, *Dalton Trans*. 2018, **47**, 4661 – 4671; (b) J. Janczak, R. Kubiak, *Inorg. Chim. Acta* 2003, **342**, 64 – 76.

15 C. G. Barraclough, A. K. Gregson and S. Mitra, *J. Chem. Phys*. 1974, **60**, 962 – 968.

16 (a) J. Janczak, R. Kubiak, M. Śledź, H. Borrmann and Y. Grin, *Polyhedron* 2003, **22**, 2689 – 2697; (b) A. L. Litvinov, A. V. Kuzmin, E. I. Yudanova, D. V. Konarev, N. R. Romanenko, S. S. Khasanov and R. N. Lyubovskaya, *Eur. J. Inorg. Chem.* 2016, 5445 – 5448.

17 (a) D. V. Konarev, A. V. Kuzmin, S. V. Simonov, S. S. Khasanov, A. Otsuka, H. Yamochi, G. Saito and R. N. Lyubovskaya, *Dalton Trans*. 2012, **41**, 13841 – 13847; (b) D. V. Konarev, S. S. Khasanov, M. Ishikawa, A. Otsuka, H. Yamochi, G. Saito and R. N. Lyubovskaya, *Inorg. Chem*. 2013, **52**, 3851 – 3859; (c) D. V. Konarev, A. V. Kuzmin, S. S. Khasanov and R. N. Lyubovskaya, *Dalton Trans*. 2013, **42**, 9870 – 9876; (d) D. V. Konarev, L. V. Zorina, S. S. Khasanov, E. U. Hakimova and R. N. Lyubovskaya, *New J. Chem*. 2012, **6**, 48 – 51.

18 N. F. Chilton, R. P. Anderson, L. D. Turner, A. Soncini and K. S. Murray, *J. Comput. Chem.*, 2013, **34**, 1164–1175. PHI can be downloaded from the link: http://nfchilton.com/phi.html.

19 L. Escriche-Tur, M. Font-Bardia, B. Albela and M. Corbella, *Dalton Trans*, 2017, **46**, 2699 – 2714.

20 (a) C. Mantel, C. Baffert, I. Romero, A. Deronzier, J. Pécaut, M.-N. Collomb and C. Duboc, *Inorg. Chem*. 2004, **43**, 6455 – 6463; (b) C. Duboc, M.-N. Collomb and F. Neese, *Appl. Magn. Reson.* 2010, **37**, 229 – 245.

21 C. Benelli and D. Gatteschi, *Chem. Rev.* 2002, **102**, 2369 – 2387.

22 (a) K. R. Meihaus, M. E. Fieser, J. F. Corbey, W. J. Evans and J. R. Long, *J. Am. Chem. Soc*. 2015, **137**, 9855 – 9860; (b) W. W. Lukens, M. Speldrich, P. Yang, T. J. Duignan, J. Autschbach and P. Kögerler, *Dalton Trans*. 2016, **45**, 11508 – 11521.

23 (a) R. D. Rogers, R. Vann Bynum and J. L. Atwood, *J. Organomet. Chem*. 1980, **192**, 65 – 73; (b) U. Baisch, S. Pagano, M. Zeuner, N. Barros, L. Maron and W. Schnick, *Chem. Eur. J.* 2006, **12**, 4785 – 4798; (c) F. Benetollo, G. Bombieri, C. Bisi Castellani, W. Jahn and R.D. Fischer, *Inorg. Chim. Acta,* 1984, **95**, L7-L10.

24 (a) J. O. Moilanen, N. F. Chilton, B. M. Day, T. Pugh and R. A. Layfield, *Angew. Chem. Int. Ed*. 2016, **128**, 5611 – 5615; (b) M. V. Mikhailenko, S. S. Khasanov, A. F. Shestakov, A. V. Kuzmin, A. Otsuka, H. Yamochi, H. Kitagawa and D. V. Konarev, *Chem. Eur. J.* 2022, **28**, e202104165.

Synopsis for TOC

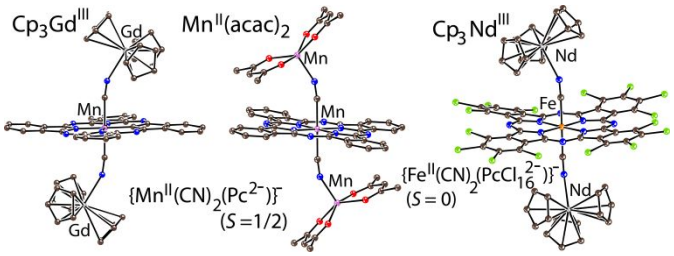

Cyanation of $Mn^{II}Pc$, $Fe^{II}Pc$ or $Fe^{II}PcCl_{16}$ yields $\{Cryptand(K^+)\}_2\{M^{II}(CN)_2(macrocycle^{2-})\}^{2-}\cdot XC_6H_4Cl_2$ (M^{II} = Mn^{II} and Fe^{II}, X = 1 and 2) complexes. Dicyano-complexes are used to obtain trinuclear assemblies in $\{Cryptand(K^+)\}_2\{M^{II}(CN)_2Pc\cdot(MF)_2\}^{2-}\cdot nC_6H_4Cl_2$ (M^{II} = Mn^{II}, Fe^{II}) where MF is manganese(II) acetylacetonate (S = 5/2), tris(cyclopentadienyl)gadolinium(III) (S = 7/2) or neodymium(III) (S = 3/2). Optical and magnetic properties of these assemblies are discussed.

ARTICLE

Trinuclear coordination assemblies of low-spin dicyano manganese(II) (*S* = 1/2) and iron(II) (*S* = 0) phthalocyanines with manganese(II) acetylacetonate and tris(cyclopentadienyl)gadolinium(III) and neodymium(III)

Received 00th January 20xx,
Accepted 00th January 20xx

DOI: 10.1039/x0xx00000x

Nikita R. Romanenko,[a] Alexey V. Kuzmin,[b] Maxim V. Mikhailenko,[a] Maxim A. Faraonov,[a] Salavat S. Khasanov,[c] Evgeniya I. Yudanova,[a] Alexander F. Shestakov,[a] Akihiro Otsuka,[c, d] Hideki Yamochi,[c, d] Hiroshi Kitagawa,[c] and Dmitri V. Konarev[a*]

Reaction of $Mn^{II}Pc$, $Fe^{II}Pc$ or $Fe^{II}PcCl_{16}$ with KCN in the presence of cryptand[2.2.2] yielded dicyano-complexes $\{Cryptand(K^+)\}_2\{M^{II}(CN)_2(macrocycle^{2-})\}^{2-}\cdot XC_6H_4Cl_2$ (M = Mn and Fe, X = 1 and 2) that were used for the preparation of trinuclear assemblies of general formula $\{Cryptand(K^+)\}_2\{M^{II}(CN)_2Pc\cdot(ML)_2\}^{2-}\cdot nC_6H_4Cl_2$ (M^{II} = Mn^{II}, Fe^{II}; n = 1, 4 and 5). These assemblies were formed via coordination of two manganese(II) acetylacetonate (ML = $Mn^{II}(acac)_2$, *S* = 5/2), tris(cyclopentadienyl)gadolinium (ML = Cp_3Gd^{III}, *S* = 7/2) or tris(cyclopentadienyl)neodymium (ML = Cp_3Nd^{III}, *S* = 3/2) units to nitrogen atoms of bidentate cyano ligands. The N(CN)-Mn{$Mn^{II}(acac)_2$} bond is 2.129(3) Å long but the bonds are elongated to 2.43-2.49 Å for tris(cyclopentadienyl)lanthanides. $\{Cryptand(K^+)\}_2\{Mn^{II}(CN)_2Pc\cdot(Mn^{II}(acac)_2)_2\}^{2-}\cdot 5C_6H_4Cl_2$ (2) contains three Mn(II) ions in different spin states (*S* = 5/2 and 1/2). Strong antiferromagnetic coupling of spins observed between them with exchange interaction (*J*) of -17.6 cm^{-1} providing the formation of high *S* = 9/2 spin state for $\{Mn^{II}(CN)_2Pc\cdot(Mn^{II}(acac)_2)_2\}^{2-}$ dianions at 2 K. Estimated exchange interaction between Mn^{II} (*S* = 1/2) and Gd^{III} (*S* =7/2) spins in $\{Mn^{II}(CN)_2Pc\cdot(Cp_3Gd^{III})_2\}^{2-}$ is only -1.1 cm^{-1}, and in contrast to **2**, nearly independent Gd^{III} and Mn^{II} centers are formed. As a result, no transition to the high-spin state is observed in these dianions. The $\{Mn^{II}(CN)_2Pc\cdot(Cp_3Nd^{III})_2\}^{2-}$ and$\{Fe^{II}(CN)_2Pc\cdot(Cp_3Nd^{III})_2\}^{2-}$ dianions with Cp_3Nd^{III} show the decrease of $\chi_M T$ values in the whole studied temperature range (300-1.9 K). Similar behaviour was found previously for pristine Cp_3Nd^{III} and $Cp_3Nd^{III}\cdot L$ complexes (L = alkylisocyanide ligand).

Introduction

Metallophthalocyanines (MPcs) present a large family of compounds which are used as dyes, sensors and materials for electronic and photoelectronic devices and solar cells.[1,2] Due to stacked or layered arrangement in the crystals MPcs can show high conductivity by partial oxidation of the macrocycles. Partial oxidation of $\{Fe^{III}(CN)_2(Pc^{2-})\}^-$ yields a compound showing giant magnetoresistance. In this case the interaction of conducting π-electrons delocalized over the macrocycles with *d*-electrons located on Fe^{III} atoms (*S* = 1/2) occurs providing the effect of magnetic field on conductivity.[3] MPcs can also be used as building blocks in the design of assemblies with promising optical and magnetic properties. Indigo and thioindigo dianions coordinate to central metal atoms of MPcs thereby combining phthalocyanine and organic dye in one molecule[4]. Such assemblies can show thermoinduced charge transfer between ligands[5]. Magnetic properties of MPcs can be modified by an addition of metal-containing fragments bearing heteroatoms or cyano-ligands to central metal atoms of MPcs. The examples of such fragments are $\{CpFe^{III}(dppe)CN\}^+$, $\{CpRu^{III}(dppe)CN\}^+$, $\{CpCo^{III}[(MeO)_2PO^-]_3\}^-$ and others.[6] Another promising way is an addition of metal-containing fragments to tin(II) or indium(III) phthalocyanines. This coordination is possible due to the formation of stable Sn(In)-M σ-bonds. In this case unpaired electrons are positioned either on the radical trianion $Pc^{\bullet 3-}$ macrocycles or coordinated metal atoms (M). Different fragments (M) can be attached as follows: $Fe(CO)_4$, $CpMo(CO)_2$, Cp^*RhCl_2, Cp^*IrCl_2, $CpFe(CO)_2$, $Ru_3(CO)_{11}$, $Os_3(CO)_{10}Cl$ and others.[7]

[a] *Institute of Problems of Chemical Physics RAS, Chernogolovka, Moscow region, 142432 Russia;*
[b] *Institute of Solid State Physics RAS, Chernogolovka, Moscow region, 142432 Russia;*
[c] *Division of Chemistry, Graduate School of Science, Kyoto University, Sakyo-ku, Kyoto 606-8502, Japan;*
[d] *Research Center for Low Temperature and Materials Sciences, Kyoto University, Sakyo-ku, Kyoto 606-8501, Japan.*

Electronic Supplementary Information (ESI) available: Supporting Information is available free of charge on the website. Experimental section including materials, general, synthesis and X-ray crystal structure determination, IR spectra of starting compounds and **1**-**8**, UV-visible-NIR spectra of **5** and **6**, crystal structures of **2**, **3** and **7**, **8**, details of magnetic measurements for **1-4, 6, 7** and results of theoretical calculations for **1** and **2**. See DOI: 10.1039/x0xx00000x

In this work dicyano complexes of manganese(II) and iron(II) phthalocyanines as well as iron(II) hexadecachlorophthalocyanine have been obtained and studied. Such complexes are known for manganese(II)[8] and (III)[9], as well as iron(II) and (III) phthalocyanines[10] but they have not been investigated for iron(II) hexadecachlorophthalocyanine so far. In this work we present for the first time temperature dependent EPR and SQUID measurements for the $\{Mn^{II}(CN)_2Pc\}^{2-}$ dianions. The $\{M^{II}(CN)_2Pc\}^{2-}$ dianions are used to obtain trinuclear assemblies $\{M^{II}(CN)_2Pc\cdot(ML)_2\}^{2-}$ with two manganese(II) acetylacetonate, tris(cyclopentadyenyl)gadolinium(III) or neodymium(III) as metal-containing ML units. Essential antiferromagnetic coupling between high- (S = 5/2) and low- (S = 1/2) spin manganese(II) atoms in $\{Mn^{II}(CN)_2Pc\cdot[Mn^{II}(acac)_2]_2\}^{2-}$ provides a transition of these units to high-spin (S = 9/2) state. Compounds with the $\{Mn^{II}(CN)_2Pc\cdot(Cp_3Gd^{III})_2\}^{2-}$, $\{Mn^{II}(CN)_2Pc\cdot(Cp_3Nd^{III})_2\}^{2-}$ and $\{Fe^{II}(CN)_2Pc\cdot(Cp_3Nd^{III})_2\}^{2-}$ dianions have also been obtained and studied for the first time to compare cyano-bridged assembies with d- and f-metals. Properties of $\{M^{II}(CN)_2Pc\}^{2-}$ and $\{Mn^{II}(CN)_2Pc\cdot[Mn^{II}(acac)_2]_2\}^{2-}$ dianions are discussed involving DFT calculations.

Results and discussion

a. Synthesis.

Cyanation of pristine $Mn^{II}Pc$, $Fe^{II}Pc$ and $Fe^{II}PcCl_{16}$ phthalocyanines was carried out by mixing of MPcs with an excess of KCN in the presence two equivalents of cryptand[2.2.2] in *o*-dichlorobenzene in anaerobic conditions. After one day of stirring at 60°C phthalocyanines were completely dissolved to form deep red-violet solution for $Mn^{II}Pc$ and deep green solutions for Fe(II)-containing phthalocyanines. To determine unit cell parameters for dicyano complexes we prepared their single crystals by slow mixing of the obtained solutions with *n*-hexane. Complexes **1** (M = Mn^{II}) and **5** (M = Fe^{II}) were found to be isostructural to previously studied complex $\{Cryptand(K^+)\}_2\{Sn^{IV}(CN)_2(Pc^{4-})\}^{2-}\cdot C_6H_4Cl_2$[11]. Elemental analysis of **1** supports the $\{Cryptand(K^+)\}_2\{Mn^{II}(CN)_2Pc\}^{2-}\cdot C_6H_4Cl_2$ composition which is similar to that of $\{Cryptand(K^+)\}_2\{Sn^{IV}(CN)_2(Pc^{4-})\}^{2-}\cdot C_6H_4Cl_2$. Crystal structure of isostructural complex **5** was determined from X-ray diffraction on single crystal (Fig. S14) to be $\{Cryptand(K^+)\}_2\{Fe^{II}(CN)_2Pc\}^{2-}\cdot 0.72C_6H_4Cl_2$. Structure of ~~a~~ the dicyano complex of iron(II) hexadecachlorophthalocyanine was also determined from X-ray diffraction analysis on single crystal (Table 1).

Furthermore, we studied the reaction of the $\{Mn^{II}(CN)_2Pc\}^{2-}$ dianions with two equivalents of metal acetylacetonates or tris(cyclopentadienyl)lanthanides in anaerobic conditions. Products were crystallized by slow mixing of the obtained solution with *n*-hexane allowing one to obtain single crystals suitable for X-ray diffraction analysis. Crystals with new unit cell parameters were obtained for **2**-**4** indicating the formation of new phases with trinuclear assemblies. In this case, the change in the solution color from red-violet to green was observed. In the case of (*iso*-Pr-Cp)$_3Dy^{III}$ or cobalt(II) acetylacetonate, only crystals of the starting dicyano complex were isolated, and no change in color of the solutions was found.

Table 1. Composition of the obtained complexes.

N	Composition
1	$\{Cryptand(K^+)\}_2\{Mn^{II}(CN)_2Pc\}^{2-}\cdot C_6H_4Cl_2$
2	$\{Cryptand(K^+)\}_2\{Mn^{II}(CN)_2Pc\cdot(Mn^{II}(acac)_2)_2\}^{2-}\cdot 5C_6H_4Cl_2$
3	$\{Cryptand(K^+)\}_2\{Mn^{II}(CN)_2Pc\cdot(Cp_3Gd^{III})_2\}^{2-}\cdot 4C_6H_4Cl_2$
4	$\{Cryptand(K^+)\}_2\{Mn^{II}(CN)_2Pc\cdot(Cp_3Nd^{III})_2\}^{2-}\cdot 4C_6H_4Cl_2$
5	$\{Cryptand(K^+)\}_2\{Fe^{II}(CN)_2Pc\}^{2-}\cdot 0.72C_6H_4Cl_2$
6	$\{Cryptand(K^+)\}_2\{Fe^{II}(CN)_2Pc\cdot(Cp_3Nd^{III})_2\}^{2-}\cdot 4C_6H_4Cl_2$
7	$\{Cryptand(K^+)\}_2\{Fe^{II}(CN)_2PcCl_{16}\}^{2-}\cdot 2C_6H_4Cl_2$
8	$\{Cryptand(K^+)\}_2\{Fe^{II}(CN)_2(PcCl_{16})\cdot(Cp_3Nd^{III})_2\}^{2-}\cdot C_6H_4Cl_2$

b. Crystal structures.

Geometry of $\{Mn^{II}(CN)_2Pc\}^{2-}$ has been studied in **2** and **3** whereas that of $\{Fe^{II}(CN)_2(PcCl_{16})\}^{2-}$ has been studied in **7**. Molecular structure of $\{Fe^{II}(CN)_2Pc\}^{2-}$ has also been solved in **5** but with rather low accuracy for bond lengths. Two cyano ligands coordinate to each metal atom in phthalocyanine (Fig. 1). In the case of $\{Mn^{II}(CN)_2Pc\}^{2-}$ four equatorial bonds are 1.951-1.955(3) Å but two Mn-C(CN) bonds are elongated to 2.013-2.018(3) Å (Table 2). Therefore, the Mn^{II} atoms have distorted octahedral environment. Similar geometry has been found for Fe^{II} atoms in $\{Fe^{II}(CN)_2PcCl_{16}\}^{2-}$ in which four short equatorial bonds of

Table 2. Bond lengths and angles for trinuclear assemblies studied in this work.

Coordination unit		N(CN)-M, Å	M	C(CN)-M(Pc), Å	C≡N, Å	M-N(CN)-C(CN), °	M(Pc)-N(Pc), Å	N_{meso}-C bonds (max/min length, Å)
$\{Mn^{II}(CN)_2Pc\cdot(Mn^{II}(acac)_2)_2\}^{2-}$	(**2**)	2.129(3)	Mn	2.013(3) Mn	1.156(3)	154.5(3)	1.955(3)	1.322(3) 1.328(3)
$\{Mn^{II}(CN)_2Pc\cdot(Cp_3Gd^{III})_2\}^{2-}$	(**3**)	2.433(2)	Gd	2.018(2) Mn	1.157(3)	151.5(3)	1.951(2)	1.322(3) 1.329(3)
$\{Cryptand(K^+)\}_2\{Fe^{II}(CN)_2PcCl_{16}\}^{2-}$	(**7**)	2.8747(15)	K	1.981(2) Fe	1.142(2)	147.0(3)	1.942(1)	1.320(2) 1.323(2)
$\{Fe^{II}(CN)_2(PcCl_{16})(Cp_3Nd^{III})_2\}^{2-}$	(**8**)	2.448(6) 2.491(6)	Nd Nd	1.977(7) Fe	1.143(5)	148.9(2)	1.949(5)	1.311(8) 1.328(8)

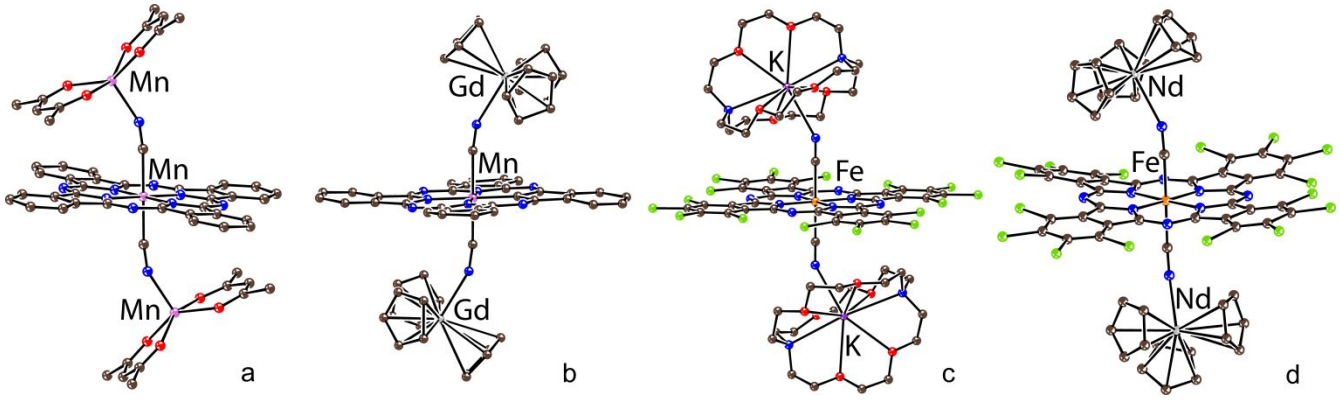

Fig. 1. Molecular structures of: (a) the $\{Mn^{II}(CN)_2Pc\cdot(Mn^{II}(acac)_2)_2\}^{2-}$ dianion in **2**; (b) the $\{Mn^{II}(CN)_2Pc\cdot(Cp_3Gd^{III})_2\}^{2-}$ dianion in **3**; (c) the neutral $\{Cryptand(K^+)\}_2\{Fe^{II}(CN)_2PcCl_{16}\}^{2-}$ assembly in **7**; (d) the $\{Fe^{II}(CN)_2(PcCl_{16})\cdot(Cp_3Nd^{III})_2\}^{2-}$ dianion in **8**.

1.942-1.949(5) Å and two longer Fe-C(CN) bonds of 1.977-1.981(2) Å are formed. Phthalocyanine macrocycles preserve dianionic state since alternation of N_{meso}-C bonds characteristic of radical trianion $Pc^{\bullet 3-}$ macrocycles[12] has not been found in **2** and **3** (Table 2). Bidentate cyano ligands in $\{Fe^{II}(CN)_2PcCl_{16}\}^{2-}$ have high affinity to metal centers since they coordinate to potassium ions in {cryptand[2.2.2](K^+)} (Fig. 1c). The K-N(CN) distance of 2.8747(15) Å is much shorter than the sum of van der Waals (vdW) radii of nitrogen and potassium atoms (4.22 Å)[13].

Metal atoms coordinate to nitrogen atoms of cyano ligands (Fig. 1). The shortest M-N(CN) bond of 2.129(3) Å length is formed with $Mn^{II}(acac)_2$. Longer M-N(CN) bonds are formed with Nd^{III} and Gd^{III} ions (2.43-2.49 Å, Table 2). In all cases coordination M-N(CN) bonds are positioned at an angle of 147-155° relative to linear NC-M-CN fragments, and total length of the assemblies is 10.2-10.8 Å. All assemblies are separated by bulky {Cryptand[2.2.2](K^+)} cations and solvent molecules (Fig. S13), and there are no direct π-π interactions between them. The shortest metal-metal distances for outer metal atoms from the adjacent assemblies are rather long being 6.25 for Nd^{III} in **8**, 6.87 for Gd^{III} in **3**, and 9.23 Å for Mn^{II} in **2**.

c. Optical properties.

Optical spectra of starting $Mn^{II}Pc$ and $Fe^{II}Pc$, and their dicyano complexes are shown in Fig. 2, whereas positions of peaks are listed in Table S5 in SI. Both $Mn^{II}Pc$ and $Fe^{II}Pc$ show spectra typical for metal(II) phthalocyanines with the Soret band at 349 and 326 nm and the Q-band at 690, 736 nm (split band) and 670 nm, respectively. Cyanation does not affect noticeably spectrum of $Fe^{II}Pc$. Only narrowing of both Soret and Q- bands is observed (Fig. 2b). On the whole, the spectrum of the $\{Fe^{II}(CN)_2Pc\}^{2-}$ dianions in **5** is similar to those of previously studied $\{Fe^{II}(N\text{-MeIm})_2Pc\}^0$ (*N*-MeIm: *N*-methylimidazole) and $\{Fe^{II}(Py)_2Pc\}^0$ complexes with low-spin Fe^{II} (S = 0).[14] On the contrary, the spectrum of $Mn^{II}Pc$ is modified substantially at cyanation. Instead of the split Q-band of $Mn^{II}Pc$, two intense bands are observed in the spectrum of **1** at 660 and 805 mn (Fig. 2a). Multiple bands are also observed at 385, 400, 451, 495, 521 and 568 nm (Fig. 2a). All these changes show that formation of $\{Mn^{II}(CN)_2Pc\}^{2-}$ affects electronic structure of $Mn^{II}Pc$. Previously, new bands were also found in the spectrum of salt with $\{Mn^{II}(CN)_2Pc\}^{2-}$ obtained by the cyanation of $Mn^{II}Pc$ in acetone.[8] Pristine $Mn^{II}Pc$ has intermediate S = 3/2 spin

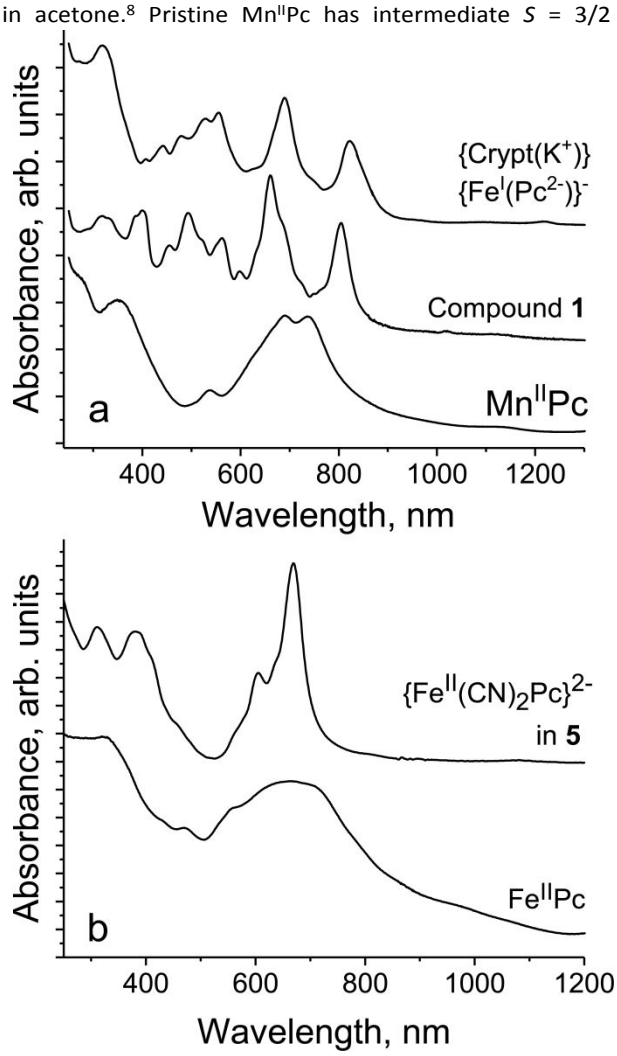

Fig. 2. UV-visible-NIR spectra of: (a) pristine $Mn^{II}Pc$ and (b) salt **1** with $\{Mn^{II}(CN)_2Pc\}^{2-}$ dianions and salt $\{Cryptand(K^+)\}\{Fe^I(Pc^{2-})\}^-\cdot C_6H_4Cl_2$ with low-spin (S = 1/2) $\{Fe^I(Pc^{2-})\}^-$ anions[17a]; (b) starting $Fe^{II}Pc$, and salt **5** with the $\{Fe^{II}(CN)_2Pc\}^{2-}$ dianions.

state.[15] This state is preserved when $Mn^{II}Pc$ forms complex with pyridine $\{Mn^{II}(Py)_2Pc\}^0$ or 1D polymer with 4,4`-bipyridyl $\{Mn^{II}(BPy)Pc\}_n$.[16] Optical spectra of these compounds support preservation of S = 3/2 spin state since they are similar to that of $Mn^{II}Pc$. Optical spectrum of $\{Mn^{II}(CN)_2Pc\}^{2-}$ supports lowering of spin state of Mn^{II} to S = 1/2 as it was observed previously[8]. It should be noted that the $\{Mn^{II}(CN)_2Pc\}^{2-}$ dianions in such configuration are isoelectronic to previously studied $\{Fe^{I}Pc\}^{-}$ anions containing Fe^{I} (S = 1/2).[17] Spectrum of $\{Cryptand(K^+)\}^+)\{Fe^{I}(Pc^{2-})\}^{-}\cdot C_6H_4Cl_2$[17a] shown in Fig. 2a is similar to that of **1** since it contains two intense bands at 688 and 822 nm, and multiple bands are manifested at 557, 526, 477, 442 and 406 nm. Both $\{M^{II}(CN)_2Pc\}^{2-}$ dianions (M = Mn^{II} and Fe^{II}) manifest a new band at 383-385 nm which is absent in the spectra of pristine phthalocyanines (Fig. 2).

The formation of assemblies does not affect noticeably the spectra of complexes containing dicyano iron(II) phthalocyanine dianions (Fig. S12 and Fig. 3b). However, coordination of metal fragments to $\{Mn^{II}(CN)_2Pc\}^{2-}$ affects its spectrum. First of all, splitting of the band at 660 nm into two bands (660 and 680 nm) is more pronounced in the spectra of **2**-**4**. An intense band at 568 nm observed in the spectrum of **1** disappears, whereas intense bands at 495 and 400 nm are blue shifted in the spectra of **2**-**4** to 473-482 and 383 nm, respectively (Fig. 3a).

IR spectra are shown in Figs. S1-S11, and positions of the peaks are listed in Tables S3 and S4. Three intense bands in the spectra of metal(II) phthalocyanines at 720-780 cm^{-1} are rather sensitive to charge state of Pc.[12] Cyanation shifts the most intense bands at 721 (Mn) and 731 cm^{-1} (Fe) to larger wavenumbers - 727 (Mn, **1**) and 734 cm^{-1} (Fe, **5**). Formation of radical trianion $Pc^{\bullet 3-}$ macrocycles shifts these bands to the opposite direction by 10-18 cm^{-1}.[12b] Therefore, coordination of two acceptor cyano ligands decreases electron density on the Pc macrocycles (the effect is opposite to the reduction). At the same time the bands attributed to the C≡N vibrations shift only slightly by 2-4 cm^{-1} at the formation of trinuclear assemblies indicating preservation of the C≡N bond length.

d. Magnetic properties.

I. Magnetic properties of $\{Mn^{II}(CN)_2Pc\}^{2-}$, $\{Fe^{II}(CN)_2Pc\}^{2-}$ and $\{Fe^{II}(CN)_2PcCl_{16}\}^{2-}$ dianions.

It is known that the $\{Mn^{II}(CN)_2Pc\}^{2-}$ dianions have the $\chi_M T$ value of 0.55 emu·K/mol indicating low-spin state (S = 1/2) of Mn^{II}.[8] We have analyzed temperature dependent magnetic characteristics of these dianions. The $\chi_M T$ value of 0.41 emu·K/mol at 300 K (Fig. 4) also corresponds to the low S = 1/2 spin state of $\{Mn^{II}(CN)_2Pc\}^{2-}$. Weiss temperature of -5 K (50-300 K) indicates weak antiferromagnetic intermolecular coupling of spins in **1** (Fig. S16). The $\chi_M T$ value only slightly decreases with temperature as shown in Fig. 4. Compound **1** manifests an intense asymmetric EPR signal in the spectrum measured for a polycrystalline sample in anaerobic conditions. It was fitted well by three Lorentzian lines with g_1 = 2.1116 (the linewidth ΔH = 8.12 mT), g_2 = 2.0746 (ΔH = 10.67 mT), g_3 = 1.9895 (ΔH = 24.33 mT) at 293 K (Fig. 5a). These components are slightly shifted and narrowed with temperature decrease down to 4.2 K: g_1 = 2.1029 (ΔH = 17.29 мТ), g_2 =2.0712 (ΔH = 9.65 mT) and g_3 =1.9907 (ΔH = 21.30 mT) (Fig. S18). The position of a signal also justifies low- (S = 1/2) spin state of Mn^{II}

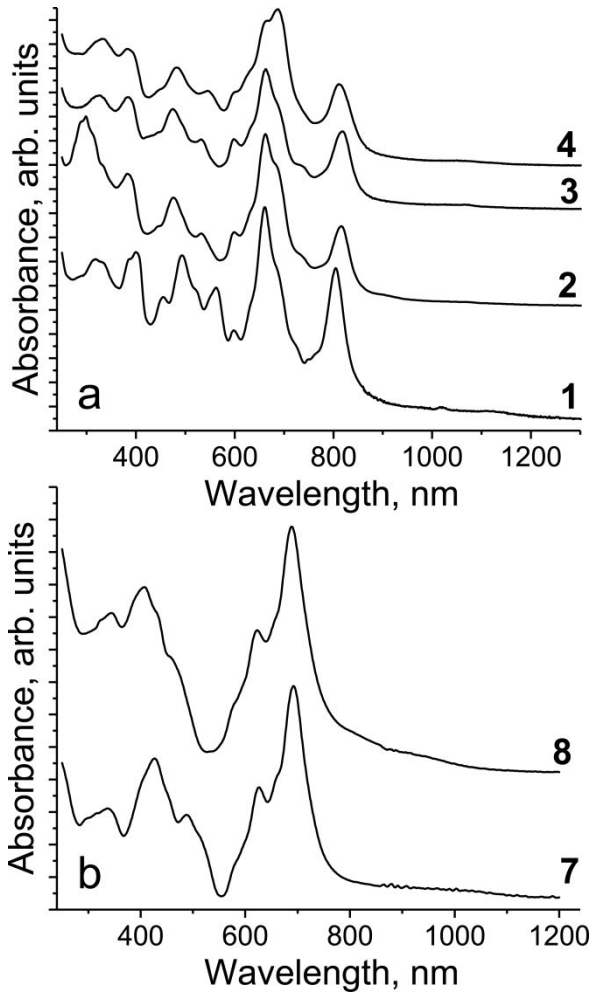

Fig, 3. UV-visible-NIR spectra of: (a) **1** with $\{Mn^{II}(CN)_2Pc\}^{2-}$ and corresponding complexes **2**, **3** and **4**; (b) **7** with $\{Fe^{II}(CN)_2PcCl_{16}\}^{2-}$ and corresponding complex **8**.

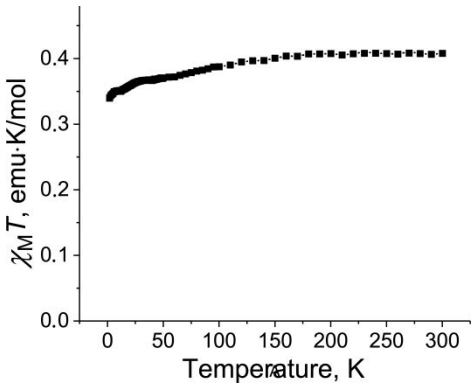

Fig. 4. Temperature dependence of $\chi_M T$ for **1** containing low-spin (S = 1/2) $\{Mn^{II}(CN)_2Pc\}^{2-}$ dianions.

in **1** since $Mn^{II}Pc$ in intermediate S = 3/2 spin state shows an asymmetric EPR signal with a low-field component at g = 4[16b].

Complexes **5** and **7** with the $\{Fe^{II}(CN)_2Pc\}^{2-}$ and $\{Fe^{II}(CN)_2PcCl_{16}\}^{2-}$ dianions have been studied by EPR technique at room and liquid helium temperatures, and **7** has also been analyzed by SQUID magnetometry. First of all, both complexes are EPR silent at these temperatures indicating singlet S = 0 spin state of the dianions. Molar magnetic susceptibility is negative and linear for **7** being χ_0 = -0.001376 emu/mol in the 50-300 K range (Fig. S36). The value of χ_0 calculated for **7** using Pascal constants is -0.001734 emu/mol. That also supports S = 0 state of $\{Fe^{II}(CN)_2PcCl_{16}\}^{2-}$. Estimated amount of Curie impurities for **7** is about 1.2% from the content of $Fe^{II}PcCl_{16}$.

II. Magnetic properties of trinuclear $\{Mn^{II}(CN)_2Pc\cdot(Mn^{II}(acac)_2)_2\}^{2-}$ assemblies in 2.

As we have shown, spin state of $\{Mn^{II}(CN)_2Pc\}^{2-}$ is S = 1/2 but manganese(II) acetylacetonate has a high-spin S = 5/2 state. As a result, the formation of a system of three independent S = 5/2, S = 1/2 and S = 5/2 spins is expected for **2** at high temperatures. The $\chi_M T$ value is 8.74 emu·K/mol at 300 K (Fig. 6, curve shown by open circles). The theoretically calculated value for such system is 9.12 emu·K/mol at g-factor = 2 that is close to the experimentally determined value. The $\chi_M T$ value

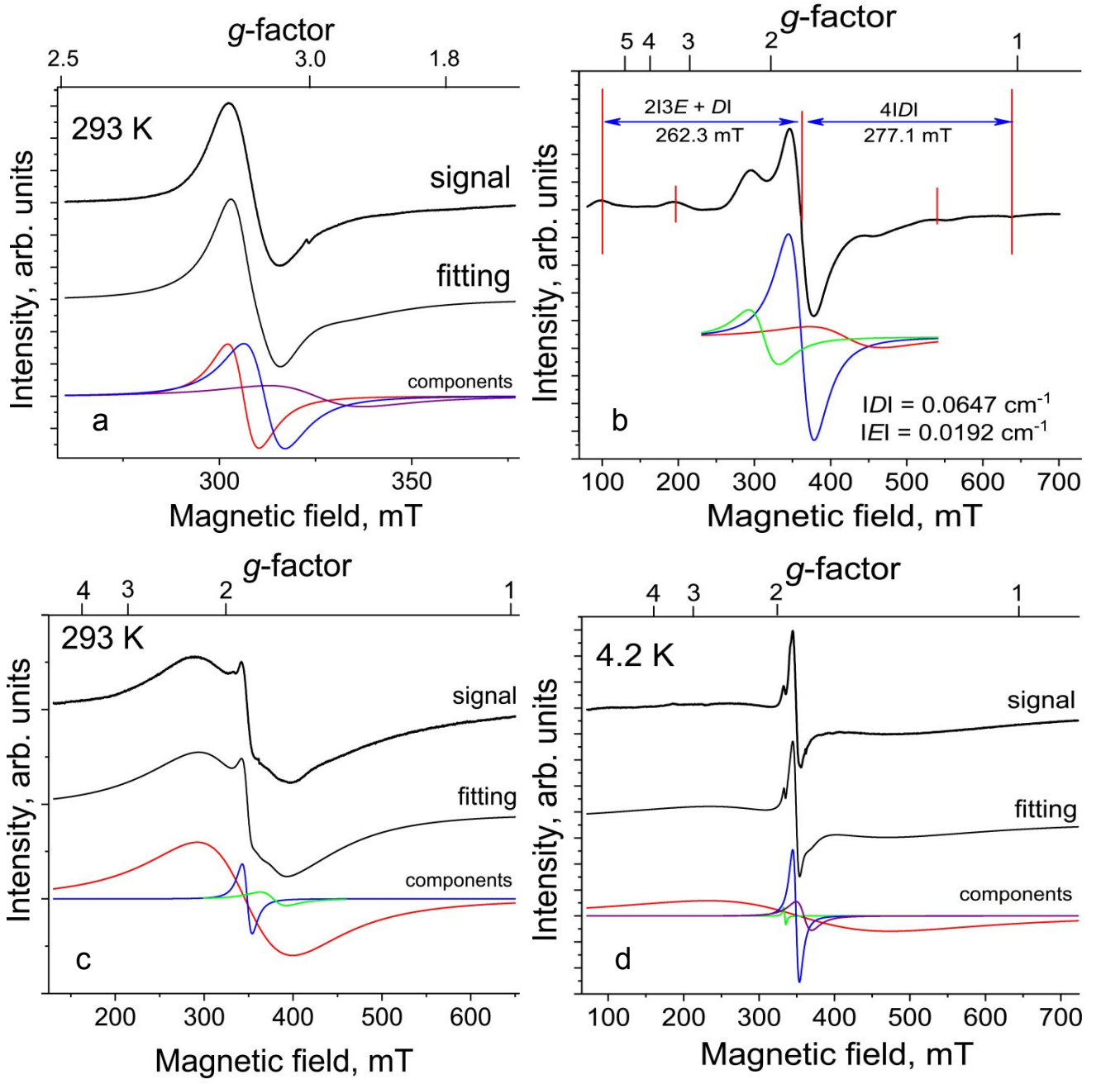

Fig. 5. Solid-state EPR spectra for the polycrystalline complexes measured in anaerobic conditions and their simulation: (a) **1** at 293 K; (b) **2** at 20 K (determination of ZFS parameters is also shown); **3** at 293 (c) and 4.2 K (d). Fitting of the signals by several Lorentzian lines is shown below the spectra.

decreases in the 50-300 K range, and Weiss temperature has been determined to be Θ = -12 K (Fig. S22) indicating antiferromagnetic coupling of spins. Magnetic behavior of **2** is modeled by PHI program[18] for three interacting Mn^{II} atoms in $\{Mn^{II}(CN)_2Pc\cdot(Mn^{II}(acac)_2)_2\}^{2-}$ with two J values as shown in Fig. 6. J_1 is for major Mn^{II} (S = 5/2) and Mn^{II} (S = 1/2) coupling and J_2 is for coupling between two boundary Mn^{II} (S = 5/2) centers located at a distance of 10.23 Å (Fig. 6). Exchange interaction J_1 = -17.6 cm^{-1} indicates strong antiferromagnetic coupling between high- and low-spin Mn^{II} atoms, whereas J_2 value is close to zero (-0.3 cm^{-1}) (-2J formalism, g = 2, Fig. 6). A small intermolecular coupling contribution of zJ' = 0.005 cm^{-1} is also taken into account (introduction of this parameter provides better correspondence between experimental and calculated curves in the 2-10 K range). Similarly, magnetic behavior of the assemblies of three high-spin (S = 5/2) Mn(II) atoms was previously modeled. In this case Mn^{II} atoms are bridged by oxygen atoms and the J_1 values in this case range from -2.1 to -2.9 cm^{-1}.[19]

Susceptibility increases below 40 K (Fig. 6) up to 11.60 emu·K/mol at 2 K. This increase can be explained by short-range magnetic ordering of spins within the assemblies since J_1 is relatively high in **2**. The value of 11.60 emu·K/mol observed at 2 K corresponds well to 12.37 emu·K/mol expected for the high S = 9/2 system at g = 2 when both S = 5/2 spins of Mn(II) are antiferromagnetically coupled with central S = 1/2 spin and, correspondingly, are ordered parallel to each other providing an S = 5/2 - 1/2 + 5/2 = 9/2 spin state. It is seen that an important condition for the manifestation of the high-spin state is a different spin state of central and outer Mn(II) atoms (S = 1/2 and S = 5/2). Field dependence of magnetization of **2** is shown in Fig. 7a. Magnetization is nearly saturated at 5T magnetic field at the value of 7.41 $N_A\mu_B$. No magnetic hysteresis is found for **2** at 2 K by susceptibility measurements in magnetic field between 5 and -5T.

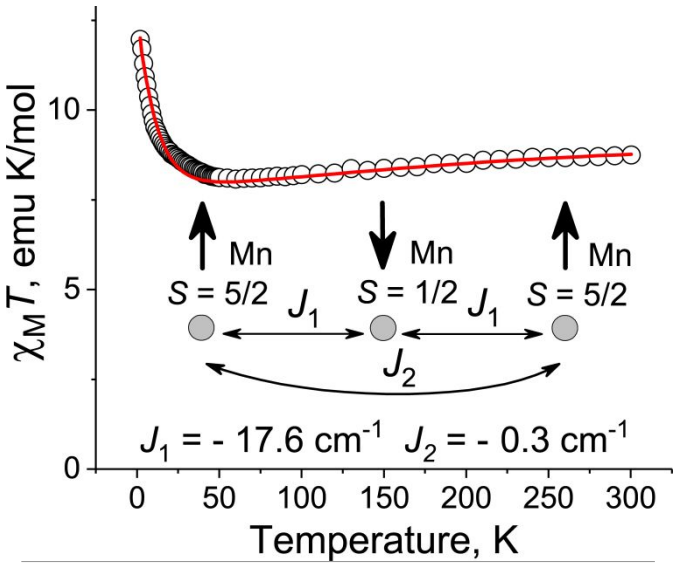

Fig. 6. Temperature dependence of χMT for {Cryptand(K+)}2{MnII(CN)2Pc·(MnII(acac)2)2}2·5C6H4Cl2 (2) in zero field cooling conditions and fitting of these data in the 2-300 K range by PHI program[18] (shown by red curve) .

Compound **2** shows an intense asymmetric EPR signal at room temperature which is fitted well by three Lorentzian lines. Parameters of these lines are g_1 = 2.0705 (ΔH = 39.2 mT), g_2 = 1.7892 (ΔH = 33.2 mT) and g_3 = 1.5410 (ΔH = 94.7 mT) at 20 K (Fig. 5b). Additional features of the EPR signal are manifested in **2** at higher and lower magnetic fields from the central three-component signal. These features can be attributed to zero-field splitting (ZFS) manifested for high-spin Mn(II) (S = 5/2) species. The following parameters can be determined: $|D|$ = 0.0647, $|E|$ = 0.0192 cm^{-1}, E/D = 0.298 and they are typical for high-spin Mn(II)[19, 20]. ZFS is not well resolved below 20 K.

c. Magnetic properties of trinuclear $\{Mn^{II}(CN)_2Pc\cdot(Cp_3Gd^{III})_2\}^{2-}$ assemblies in 3.

Cyano-bridged assemblies with tris(cyclopentadienyl)-lanthanides are still unknown, and trinuclear $\{Mn^{II}(CN)_2Pc\cdot(Cp_3Gd^{III})_2\}^{2-}$ assembly is a first example. There are two high-spin Gd^{III} atoms (S = 7/2) separated by a low-spin Mn(II) center (S = 1/2) in **3**. The $\chi_M T$ value is 15.01 emu·K/mol at 300 K (Fig 7). This value is close to that of the system with

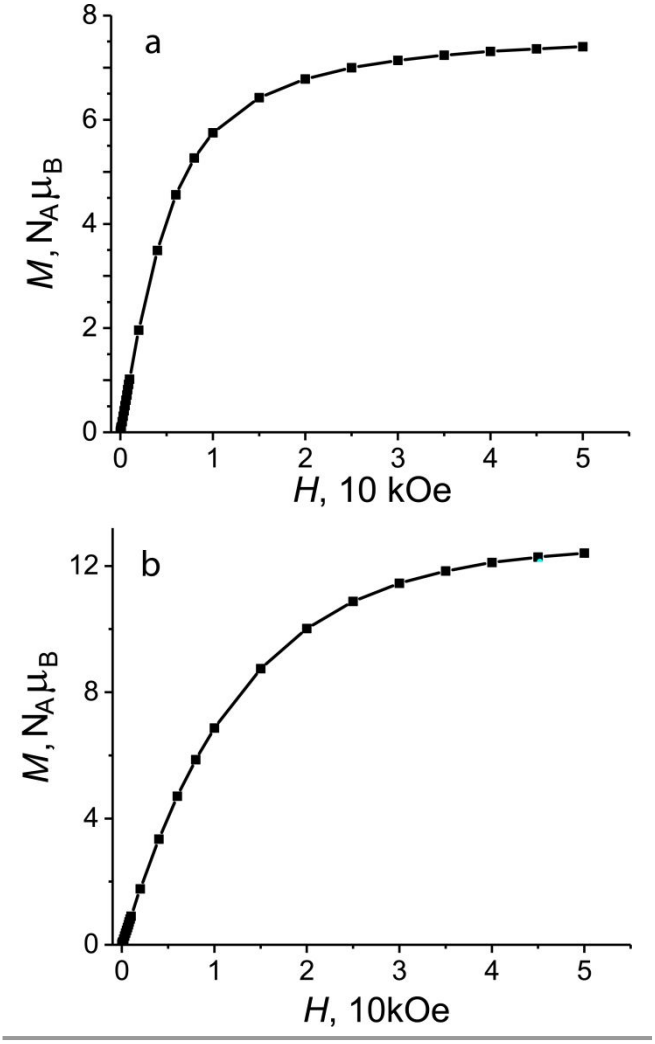

Fig.. **7**. Magnetization of **2** (a) and **3** (b) in $N_A\mu_B$ *vs* magnetic field up to 5T (black line is a guide to the eye)

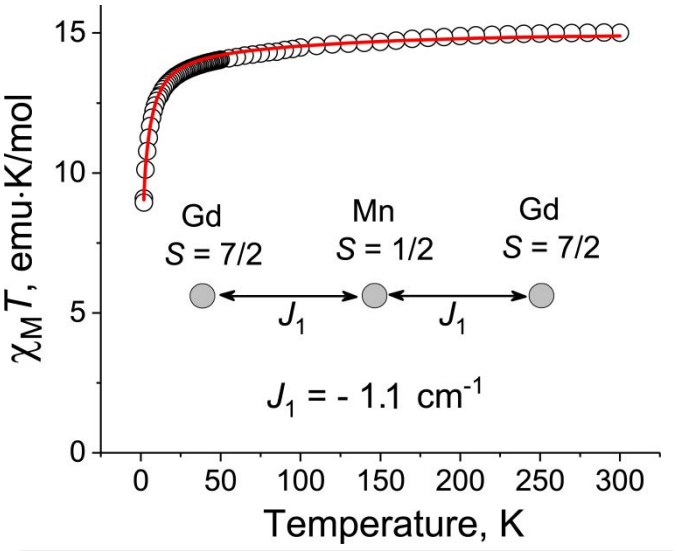

Fig. 8. (a) Temperature dependence of $\chi_M T$ for $\{Cryptand(K^+)\}_2\{Mn^{II}(CN)_2Pc\cdot(Cp_3Gd^{III})_2\}^{2-}\cdot 4C_6H_4Cl_2$ (**3**) and fitting of these data by PHI program[18] in the 1.9-300 K range (shown by red curve) .

three non-interacting S = 7/2, S = 1/2, S = 7/2 spins: 16.12 emu·K/mol at g = 2. The Gd^{III} atoms have $^8S_{7/2}$ ground state at g-factor of 2.[21]

Magnetic behavior of the trinuclear $MnGd_2$ assembly in **3** was modeled by PHI program[18] as well. A good agreement between experimental and theoretical curves is observed at very weak antiferromagnetic exchange interaction between Gd^{III} and Mn^{II} centers with J_1 = -1.1 cm^{-1} (Fig. 8). It is seen that this interaction is nearly 15 times weaker in comparison with that for **2**. Therefore, as observed previously, d-metals (Mn) provide essentially stronger magnetic coupling of spins in the cyano-bridged assemblies in comparison with f-metals (Gd). Weak coupling is also the reason of that the formation of high-spin species in not observed for **3**. Fitting for **3** was carried out at fixed g-factors of 1.84 for Mn^{II} and 1.90 for Gd^{III} which were directly extracted from the EPR spectra of 3. Zero-splitting parameter D for Gd^{III} is |0.9| cm^{-1}. Since the distance between Gd atoms from the adjacent $MnGd_2$ assemblies is 6.871 Å (Fig. S13a), a small intermolecular coupling contribution of zJ' = -0.02 cm^{-1} is also taken into account (introduction of this parameter provides better correspondence between experimental and calculated curves). The field dependence of magnetization of **3** is shown in Fig. 7b. Magnetization is not saturated even at 5T magnetic field reaching the value of 12.40 $N_A\mu_B$.

EPR spectrum of **3** at 293 K is shown in Fig. 5c. The signal contains a very wide and intense line at g_1 = 1.8699 and the linewidth of 107 mT and a substantially narrower and weaker two-component signal with g_2 = 1.7119 (ΔH = 29.4 mT), and g_3 = 1.8562 (ΔH = 11.02 mT) (Fig. 5c). Total integral intensity of the two-component narrow signal is only 2.5% from that of the wide signal and that corresponds approximately to relative contributions from two high-spin Gd^{III} atoms and low-spin Mn^{II} atoms. Therefore, the wide signal can be attributed to Gd^{III} but the narrow signal originates from Mn(II) (S = 1/2). The wide EPR signal expands greatly and shifts towards large g-factors with decreasing temperature (Figs. S28 and S29). Maximal linewidth of the signal (275 mT) at g = 1.89 is observed at 150 K, and below this temperature the signal shifts to smaller g-factors and only slightly narrows (g_1 = 1.8342 at the 242 mT linewidth, 4.2 K, Fig. 5d). The narrow signal can be fitted better by three lines at 4.2 K with g_2 = 1.7994 (20.54 mT), g_3 =1.8529 (8.90 mT), g_4 = 1.9359 (2.79 mT) (Fig. 5d). Observation of separate EPR signals from individual paramagnetic Gd^{III} and Mn^{II} species indicates weakness of magnetic coupling between them in the assemblies that is confirmed by the data obtained from SQUID magnetometry.

d. Magnetic properties of trinuclear $\{Mn^{II}(CN)_2Pc\cdot(Cp_3Nd^{III})_2\}^{2-}$ assemblies in 4.

The Nd^{III}-Mn^{II}-Nd^{III} assemblies contain two different paramagnetic centers. According to previous estimation, central Mn^{II} atom has low S = 1/2 spin state. The Nd^{III} atom in Cp_3Nd^{III} have $^4I_{9/2}$ ground state at g = 8/11. It has three 4f-electrons, and theoretical $\chi_M T$ value for Nd^{III} is expected to be 1.64 emu·K/mol.[21] However, experimentally this value is not achieved due to the population of excited states with lower total angular momentum values at room temperature.

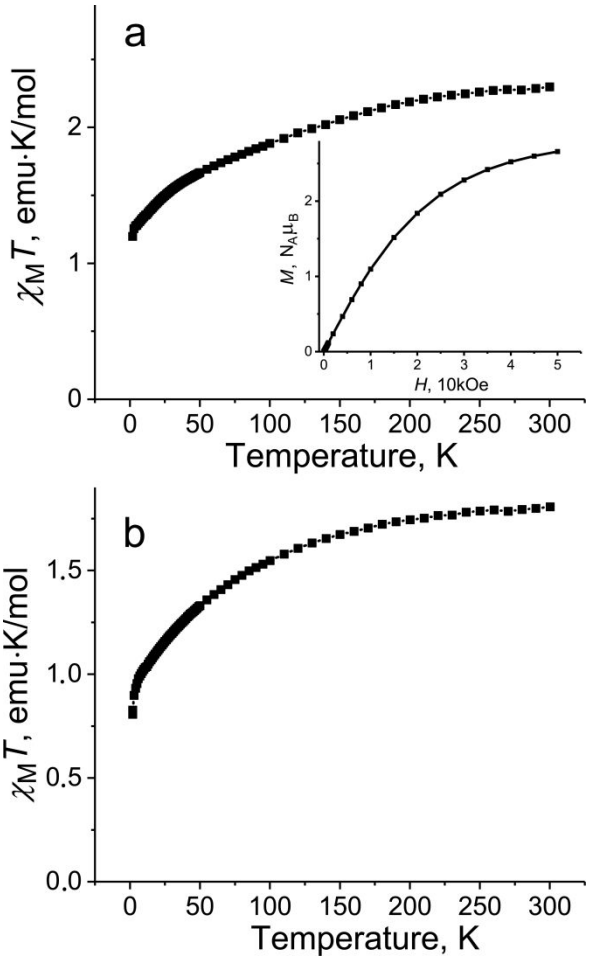

Fig. 9. Temperature dependencies of the $\chi_M T$ values for polycrystalline: **4** (a) and **6** (b). Inset for Fig. a shows magnetization of **4** in $N_A\mu_B$ *vs* magnetic field up to 5T (black line is a guide to the eye)

Previously magnetic properties of pristine Cp_3Nd^{III} as well as Cp_3Nd^{III} complexes with one alkylisocyanide ligand (L) were studied. The $\chi_M T$ values for pristine Cp_3Nd^{III} is 1.27 emu·K/mol at 300 K whereas the Cp_3Nd^{III}·L complexes show even smaller values being 0.95 emu·K/mol at 300 K. Moreover, the $\chi_M T$ value is not temperature independent even at 300 K and decreases in the 300-1.9 K range.[22] The $\chi_M T$ value for **4** is 2.30 emu·K/mol at 300 K which is also lower than expected (3.56 emu·K/mol) for three non-interacting centers: two Nd^{III} atoms in $^4I_{9/2}$ ground state and low-spin Mn^{II} ion (S = 1/2) (Fig 8a). This value decreases to 1.125 emu·K/mol at 1.9 K in the whole studied temperature range (300-1.9 K, Fig 8a). Similarly to Cp_3Nd^{III} and Cp_3Nd^{III}·L[22], this decrease can be attributed to the crystal field effects for Nd^{III} and additional contribution for **4** can be given also by weak antiferromagnetic coupling between the Nd^{III} and Mn^{II} centers within the assemblies. The compound with the $\{Fe^{II}(CN)_2Pc\cdot(Cp_3Nd^{III})_2\}^{2-}$ dianions (**6**) was also synthesized. In this case the Fe^{II} atoms in phthalocyanine are diamagnetic (S = 0), and the exchange through them is weaker due to a long distance between two Nd^{III} atoms (about 10.8 Å for isostructural **3**). Therefore, in contrast to **4**, magnetic behavior of **6** is defined mainly by the isolated $Cp_3Nd^{III}(NC)$ centers. The $\chi_M T$ value of 1.92 emu·K/mol at 300 K for **6** (Fig. 8b) is lower than that for **4** (Fig. 8a) justifying the presence of an additional paramagnetic center Mn^{II} (S = 1/2) in **4**. The $\chi_M T$ value decreases with temperature down to 0.75 emu·K/mol at 1.9 K (Fig. 8b), and such behavior is similar to those of **4**, Cp_3Nd^{III} and Cp_3Nd^{III}·L[21]. The field dependence of magnetization of **4** is shown in Fig. 9a, inset. Magnetization is not saturated even at 5T magnetic field reaching the value of 2.67 $N_A\mu_B$.

EPR spectrum of **4** was studied in the 293-4.2 K range. There are wide and narrow asymmetric EPR signals which can be fitted well by several Lorentzian lines at 293 K (Fig. S33). The wide signal can be fitted by three lines with g_1 = 2.0275 (ΔH = 28.80 mT), g_2 = 2.0836 (ΔH = 10.51 mT) and g_3 = 2.1167 (ΔH = 7.52) whereas the narrow signal is fitted by two lines with g_4 = 2.0039 (ΔH = 0.32 mT) and g_2 = 2.0022 (ΔH = 0.72 mT) (Fig. S33). The latter signal is too narrow to be attributed to $\{Mn^{II}(CN)_2Pc\}^{2-}$, and its integral intensity is less than 0.1% from that of the wide signal. Therefore, most probably this signal originates from Curie impurities localized on Pc, for example, reduced $Pc^{\bullet 3-}$radical trianions but the content of these species is too low to affect magnetic properties of **4**. The wide signal can originate from both Nd^{III} and Mn^{II} species. The signal is three-component, but exact attribution of these components is not possible. Here it should be noted that Cp_3Nd^{III}·L complexes can also show EPR signals in the same range of g-factors ($g_\perp$-component)[22b]. Temperature decrease preserves the same linewidth of the components of the wide signal but they are shifted to smaller g-factors: g_1 = 1.9740 (ΔH = 24.60 mT), g_2 = 2.0519 (ΔH = 11.63 mT) and g_3 = 2.0936 (ΔH = 8.97 mT) at 4.2 K (Fig. S33).

e. Theoretical calculations.

For an isolated atom or ion with an open d-shell, the maximum multiplicity is realized according to Hund's rule. Under the influence of the ligand environment, splitting of the d-orbitals occurs and the high-spin state of the $Mn^{II}Pc$ complex with macrocyclic ligand (Fig. S39) is not realized due to strong destabilization of the x^2-y^2 orbital. Only lower axial z^2 orbital is populated in the ground quartet state. The sextet and doublet states are higher in energy by 0.53 and 1.12 eV, respectively. Upon coordination of two axial cyano-ligands in $\{Mn^{II}(CN)_2Pc\}^{2-}$ (Fig. S39), relative energy of the z^2 orbital increases. Therefore, the low-spin doublet state of the $\{Mn^{II}(CN)_2Pc\}^{2-}$ complex is a ground state (Fig. 10), and quartet and sextet states are higher by 0.48 and 1.24 eV, respectively. For similar reasons, the $\{Fe^{II}(CN)_2Pc\}^{2-}$ dianion (Fig. S40) has a singlet ground state, and a triplet one is higher by 0.81 eV.

$Mn^{II}(acac)_2$ coordination to nitrogen atoms of cyano ligands has almost no effect on geometry of the central $\{Mn^{II}(CN)_2Pc\}^{2-}$ fragment (see Fig. S42). In this case, the charge on a cyano ligand decreases from -0.488 to -0.234. At the same time, comparable electron density transfer of -0.382 occurs mainly from the macrocycle since the charge on the central Mn^{II} atom changes only slightly from 0.171 to 0.153. A slight decrease in the Mn-C(CN) distance from 2.031 to 1.998 Å ~~at~~ upon coordination of $Mn^{II}(acac)_2$ can be attributed to the donor-acceptor transfer of electron density (-0.445) to each $Mn^{II}(acac)_2$ unit. The $\{Mn^{II}(CN)_2Pc\cdot(Mn^{II}(acac)_2)_2\}^{2-}$ dianions can have high- (S = 11/2) and low- (S = 9/2) spin states at parallel and antiparallel arrangement of spins of high- and low-spin Mn^{II} atoms. These states are nearly degenerated, and their relative energies are discussed in SI.

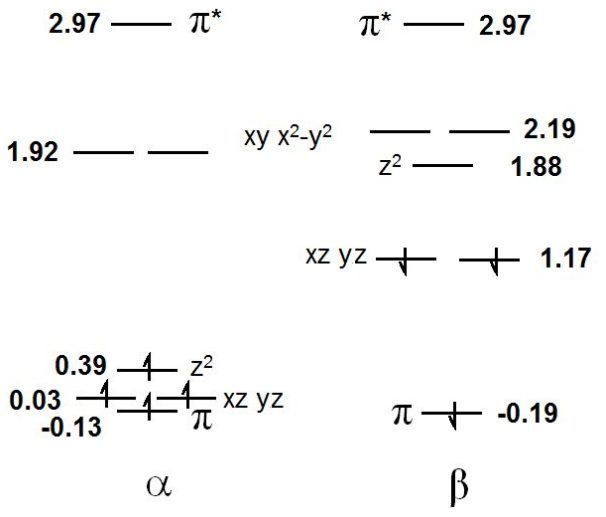

Fig. 10. Scheme of electronic levels calculated for the $\{Mn^{II}(CN)_2Pc\}^{2-}$ dianions. Energies are given in eV.

Conclusion

The dicyano complexes of $Mn^{II}Pc$, $Fe^{II}Pc$ and $Fe^{II}PcCl_{16}$ have been obtained. Central metal atoms decrease spin state to the lowest possible state (S = 1/2 for Mn^{II} and S = 0 for Fe^{II}-containing complexes). The formation of $\{Mn^{II}(CN)_2Pc\}^{2-}$ provides appearance of new bands in the visible and NIR ranges. As a result, their spectra show some similarities with optical spectrum of isoelectronic $\{Fe^{I}(Pc^{2-})\}^{-}$ anions. These dicyano complexes have been used for preparation of trinuclear assemblies with $Mn^{II}(acac)_2$ as well as Cp_3Gd^{III} and Cp_3Nd^{III}. It should be noted that tris(cyclopentadienyl)-lanthanides are used for preparation of cyano-bonded assemblies for the first time, and this approach opens a new

way for the development of lanthanide-containing assembles. Previously, mainly neutral ligands were coordinated to tris(cyclopentadienyl)gadolinium(III) and neodymium(III)[22b, 23]. Antiferromagnetic coupling of high-spin Mn^{II} (S = 5/2) with central low-spin Mn^{II} (S =1/2) orders spins of outer atoms parallel to each other producing high-spin S = 9/2 $\{Mn^{II}(CN)_2Pc\cdot(Mn^{II}(acac)_2)_2\}^{2-}$ dianions at 2 K. Previously, high-spin state was found for the assemblies of radical anions or trianions of substituted hexaazatriphenylenes with three paramagnetic metal centers like Co^{II} (S = 3/2) or Fe^{II} (S = 2). In this case spins of metal atoms are ordered parallel to each other when they couple antiferromagnetically with S = 1/2 spin of hexaazatriphenylenes.[24] This work shows that trinuclear assemblies containing metal ions in high- and low-spin states can also form similar high-spin species. They are promising building blocks to prepare compounds with long-range magnetic ordering of spins at their close packing in the crystals or to obtain combination of conductivity and magnetism when partially oxidized or reduced phthalocyanine macrocycles are formed in such assemblies. On the contrary, essentially weaker magnetic coupling is observed between high-spin gadolinium(III) and low-spin manganese(II) atoms in $\{Mn^{II}(CN)_2Pc\cdot(Cp_3Gd^{III})_2\}^{2-}$, and in this case high-spin species are not formed down to 1.9 K.

Conflicts of interest

There are no conflicts to declare.

Acknowledgements

The work for preparation and study of **1**-**6** was supported by Russian Science Foundation (project N 21-13-00221). Study of complexes **7** and **8** with iron(II) perchlorophthalocyanine was supported by Russian Science Foundation (project N 21-73-10207). Analysis of IR spectra of **1**, **5** and **7** was supported by the Ministry of Science and Higher Education of the Russian Federation (registration number AAAA-A19-119092390079-8). Some magnetic measurements were suported by JSPS KAKENHI Grant Number JP20K05448, and the JST (ACCEL) 27 (100150500019) project.

ORCID:

M.A. Faraonov: 0000-0003-0805-601X
A. Otsuka: 0000-0002-3141-0702
H. Yamochi: 0000-0002-0127-6530
H. Kitagawa: 0000-0001-6955-3015
D.V. Konarev: 0000-0002-7326-8118

Contribution of the authors:

N.R. Romanenko -Investigation
A.V. Kuzmin -Investigation
M.V. Mikhailenko - Investigation
M.A. Faraonov - Investigation
S.S. Khasanov -Investigation
E.I. Yudanova -Formal Analysis
A.F. Shestakov - Formal Analysis
A. Otsuka - Resources
H. Yamochi -Resources
H. Kitagawa -Project administration
D.V. Konarev -Supervision Investigation Writing – original draft

Notes and references

1 (a) T. Nyokong, *Coord. Chem. Rev*. 2007, **251**, 1707 − 1722; (b) D. Placencia, W. Wang, J. Gantz, J. L. Jenkins and N. R. Armstrong, *J. Phys. Chem. C*, 2011, **115**, 18873 – 18884; (c) C. G. Claessens, W. J. Blau, M. Cook, M. Hanack, R. J. M. Nolte, T. Torres and D. Wöhrle, *Monat. Chem.* 2001, **132**, 3 − 11; (d) O. I. Koifman, T. A. Ageeva, I. P. Beletskaya, A. D. Averin, A. A. Yakushev, L. G. Tomilova, T. V. Dubinina, A. Yu. Tsivadze, Yu. G. Gorbunova, A. G. Martynov, D. V. Konarev, S. S. Khasanov, R. N. Lyubovskaya et all, *Macroheterocycles,* 2020, **13**, 311 − 467.

2 (a) L. J. Boucher, Metal Complexes of Phthalocyanines. In: G. A. Melson (eds) Coordination Chemistry of Macrocyclic Compounds. Springer, Boston, MA, 1979, pp. 461 – 516; (b) I. Beletskaya, V. S. Tyurin, A. Y. Tsivadze, R. Guilard and C. Stern, *Chem. Rev.* 2009, **109**, 1659 – 1713; (c) V. N. Nemykin and E. A. Lukyanets, *ARKIVOC,* Arkat USA, Inc., 2010, 136 – 208. DOI: http://dx.doi.org/10.3998/ark.5550190.0011.104

3 (a) J. L. Petersen, C. S. Schramm, D. R. Stojakovic, B. M. Hoffman and T. J. Marks, *J. Am. Chem. Soc.* 1977, **99**, 286 – 288; (b) D. Ethelbhert, C. Yu, M. Matsuda, H. Tajima, A. Kikuchi, T. Taketsugu, N. Hanasaki, T. Naito and T. Inabe, *J. Mater. Chem.* 2009, **19**, 718 – 723; (c) M. Matsuda, N. Hanasaki, H. Tajima, T. Naito and T. Inabe, *J. Phys. Chem. Solids* 2004, **65**, 749 – 752; (d) T. Inabe and H. Tajima, *Chem. Rev.* 2004, **104**, 5503 – 5534.

4 D. V. Konarev, A. V. Kuzmin, A. M. Fatalov, S. S. Khasanov, E. I. Yudanova and R. N. Lyubovskaya, *Chem. Eur. J.* 2018, **24**, 8415 – 8423.

5 D. V. Konarev, L. V. Zorina, S. S. Khasanov, A. F. Shestakov, A. M. Fatalov, A. Otsuka, H. Yamochi, H. Kitagawa and R. N. Lyubovskaya, *Inorg. Chem*. 2018, **57**, 583 – 589.

6 (a) M. T. M. Choi, C.-F. Choi and D. K. P. Ng, *Tetrahedron*, 2004, **60**, 6889–6894; (b) J. Silver, J. L. Sosa-Sanchez and C. S. Frampton, *Inorg. Chem.* 1998, **37**, 411 – 417; (c) A. Geiss, H. Vahrenkamp, *Inorg. Chem.* 2000, **39**, 4029 – 4036; (d) H. Ke, W.-K. Wong, W.-Y. Wong, H.-L. Tam, C.-T. Poon and F. Jiang, *Eur. J. Inorg. Chem.* 2009, 1243 – 1247; (e) Y. Z. Voloshin, O. A. Varzatskii, S. V. Korobko, V. Y. Chernii, S. V. Volkov, L. A. Tomachynski, V. I. Pehn'o, M. Yu. Antipin and Z. A. Starikova, *Inorg. Chem.* 2005, **44**, 822 – 824; (f) S. V. Dudkin, A. S. Belov, Y. V. Nelyubina, A. V. Savchuk, A. A. Pavlov, V. V. Novikova, Y. Z. Voloshin, *New J. Chem*. 2017, **41**, 3251 – 3259; (g) A. Geiss, M. J. Kolm, C. Janiak and H. Vahrenkamp, *Inorg. Chem.* 2000, **39**, 4037 – 4043.

7 (a) D. V. Konarev, A. V. Kuzmin, Y. Nakano, M. A. Faraonov, S. S. Khasanov, A. Otsuka, H. Yamochi, G. Saito and R. N. Lyubovskaya, *Inorg. Chem.* 2016, **55**, 1390 – 1402; (b) D. V. Konarev, A. V. Kuzmin, M. S. Batov, S. S. Khasanov, A. Otsuka, H. Yamochi, H. Kitagawa and R. N. Lyubovskaya, *ACS Omega* 2018, **3**, 14875 – 14888; (c) N. R. Romanenko, A. V. Kuzmin, S. S. Khasanov, M. A. Faraonov, E. I. Yudanova, Y. Nakano, A. Otsuka, H. Yamochi, H. Kitagawa and D. V. Konarev, *Dalton Trans*, 2022, **51**, 2226 – 2237.

8 S. Sievertsen, H. Grunewald and H. Homborg, *Z. Anorg. Allg. Chem*., 1993, **619**, 1729 – 1737.

9 (a) A. P. Hansen and H. M. Goff, *Inorg. Chem.* 1984, **23**, 4519 – 4525; (b) M. Matsuda, J.-I. Yamaura, H. Tajima and T. Inabe, *Chem. Let*. 2005, **34**, 1524 – 1525.

10 (a) B. W. Dale, *Trans. Faraday Soc*. 1969, 331 – 338; (b) M. J. Stillman and A. J. Thomson, *J. Chem. Soc., Faraday Trans. 2*, 1974, **70**, 790–804; (c) T. Nyokong, *J. Chem. Soc. Dalton Trans*, 1993, 3601 – 3604; (d) M. Matsuda, T. Asari, T. Naito, T. Inabe, N. Hanasaki, and H.Tajima, *Bull. Chem. Soc. Jpn.* 2003, **76**, 1935 – 1940.

11 D. V. Konarev, A. V. Kuzmin, A. F. Shestakov, I. A. Rompanen

and R. N. Lyubovskaya, *Dalton Trans*, 2020, **49**, 16801 – 16812.
12 12 (a) J. A. Cissell, T. P. Vaid and A. L. Rheingold, *Inorg. Chem.* 2006, **45**, 2367 – 2369; (b) D. V. Konarev, A. V. Kuzmin, M. A. Faraonov, M. Ishikawa, Y. Nakano, S. S. Khasanov, A. Otsuka, H. Yamochi, G. Saito and R. N. Lyubovskaya, *Chem. Eur. J.* 2015, **21**, 1014 – 1028; (c) D. V. Konarev, M. A. Faraonov, A. V. Kuzmin, S. S. Khasanov, Y. Nakano, M. S. Batov, S. I. Norko, A. Otsuka, H. Yamochi, G. Saito and R. N. Lyubovskaya, *New J. Chem.* 2017, **41**, 6866 – 6874; (d) D. V. Konarev, A. V. Kuzmin, S. S. Khasanov, A. L. Litvinov, A. Otsuka, H. Yamochi, H. Kitagawa and R. N. Lyubovskaya, *Chem. Asian J.* 2018, **13**, 1552 – 1560; e). D. V. Konarev, A. V. Kuzmin, S. S. Khasanov, M. S. Batov, A. Otsuka, H. Yamochi, H. Kitagawa and R. N. Lyubovskaya, *CrystEngComm*. 2018, **20**, 385 – 401.
13 S. S. Batsanov, *Inorg. Mat.* 2001, **37**, 871 – 885.
14 (a) D. V. Konarev, A. V. Kuzmin, Y. Nakano, S. S. Khasanov, A. Otsuka, H. Yamochi, H. Kitagawa and R. N. Lyubovskaya, *Dalton Trans*. 2018, **47**, 4661 – 4671; (b) J. Janczak, R. Kubiak, *Inorg. Chim. Acta* 2003, **342**, 64 – 76.
15 C. G. Barraclough, A. K. Gregson and S. Mitra, *J. Chem. Phys*. 1974, **60**, 962 – 968.
16 (a) J. Janczak, R. Kubiak, M. Śledź, H. Borrmann and Y. Grin, *Polyhedron* 2003, **22**, 2689 – 2697; (b) A. L. Litvinov, A. V. Kuzmin, E. I. Yudanova, D. V. Konarev, N. R. Romanenko, S. S. Khasanov and R. N. Lyubovskaya, *Eur. J. Inorg. Chem.* 2016, 5445 – 5448.
17 (a) D. V. Konarev, A. V. Kuzmin, S. V. Simonov, S. S. Khasanov, A. Otsuka, H. Yamochi, G. Saito and R. N. Lyubovskaya, *Dalton Trans*. 2012, **41**, 13841 – 13847; (b) D. V. Konarev, S. S. Khasanov, M. Ishikawa, A. Otsuka, H. Yamochi, G. Saito and R. N. Lyubovskaya, *Inorg. Chem*. 2013, **52**, 3851 – 3859; (c) D. V. Konarev, A. V. Kuzmin, S. S. Khasanov and R. N. Lyubovskaya, *Dalton Trans*. 2013, **42**, 9870 – 9876; (d) D. V. Konarev, L. V. Zorina, S. S. Khasanov, E. U. Hakimova and R. N. Lyubovskaya, *New J. Chem*. 2012, **6**, 48 – 51.
18 N. F. Chilton, R. P. Anderson, L. D. Turner, A. Soncini and K. S. Murray, *J. Comput. Chem.*, 2013, **34**, 1164–1175. PHI can be downloaded from the link: http://nfchilton.com/phi.html.
19 L. Escriche-Tur, M. Font-Bardia, B. Albela and M. Corbella, *Dalton Trans*, 2017, **46**, 2699 – 2714.
20 (a) C. Mantel, C. Baffert, I. Romero, A. Deronzier, J. Pécaut, M.-N. Collomb and C. Duboc, *Inorg. Chem*. 2004, **43**, 6455 – 6463; (b) C. Duboc, M.-N. Collomb and F. Neese, *Appl. Magn. Reson.* 2010, **37**, 229 – 245.
21 C. Benelli and D. Gatteschi, *Chem. Rev.* 2002, **102**, 2369 – 2387.
22 (a) K. R. Meihaus, M. E. Fieser, J. F. Corbey, W. J. Evans and J. R. Long, *J. Am. Chem. Soc*. 2015, **137**, 9855 – 9860; (b) W. W. Lukens, M. Speldrich, P. Yang, T. J. Duignan, J. Autschbach and P. Kögerler, *Dalton Trans*. 2016, **45**, 11508 – 11521.
23 (a) R. D. Rogers, R. Vann Bynum and J. L. Atwood, *J. Organomet. Chem*. 1980, **192**, 65 – 73; (b) U. Baisch, S. Pagano, M. Zeuner, N. Barros, L. Maron and W. Schnick, *Chem. Eur. J.* 2006, **12**, 4785 – 4798; (c) F. Benetollo, G. Bombieri, C. Bisi Castellani, W. Jahn and R.D. Fischer, *Inorg. Chim. Acta,* 1984, **95**, L7-L10.
24 (a) J. O. Moilanen, N. F. Chilton, B. M. Day, T. Pugh and R. A. Layfield, *Angew. Chem. Int. Ed*. 2016, **128**, 5611 – 5615; (b) M. V. Mikhailenko, S. S. Khasanov, A. F. Shestakov, A. V. Kuzmin, A. Otsuka, H. Yamochi, H. Kitagawa and D. V. Konarev, *Chem. Eur. J.* 2022, **28**, e202104165.